BPSK Based Super Regenerative Receiver

Deepak Shastry Ravishankar

Master of Science Thesis

Electrical Engineering
Department of Telecommunications
Faculty of Electrical Engineering, Mathematics and Computer Science
Delft University of Technology

TU Delft
Delft
University of
Technology

Wireless and Mobile Communications

July 9, 2012

BPSK Based Super Regenerative Receiver

Master of Science Thesis

For the degree of Master of Science in
Electrical Engineering
at Delft University of Technology

Deepak Shastry Ravishankar

July 9, 2012

Faculty of Electrical Engineering, Mathematics and Computer Science
Delft University of Technology
Delft, The Netherlands

The work in this thesis was done at IMEC Holst Centre.

Delft University of Technology
Department of
Telecommunications

The undersigned hereby certify that they have read and recommend to the Faculty of Electrical Engineering, Mathematics and Computer Science for acceptance a thesis entitled

BPSK Based Super Regenerative Receiver

by

Deepak Shastry Ravishankar

in partial fulfillment of the requirements for the degree of

Master of Science.

Dated: July 9, 2012

Supervisor:

Dr.ir. G.J.M. Janssen

Readers:

Dr. Li Huang

Dr. O.A. Krasnov

Abstract

The Super Regenerative Receiver was invented by Armstrong in 1922 [1]. It is used in various applications such as sensor networks, short distance telemetry, home automation, biomedicine, remotely controlled systems, etc., because of its simplicity and low power design. In the classical super regenerative receiver, the RF oscillations obtained at the output of the oscillator is applied to a non-linear detector followed by a low pass filter.
Hence the demodulation capabilities of the super regenerative receiver was restricted to amplitude modulation or on off keying (OOK) signals.
The challenge is to use the super regenerative architecture to demodulate phase modulated signals which are more robust to interference compared to OOK signals and still maintaining the low power, low cost features of the receiver. The principle of super regenerative receiver is based on the theory of quenching, where a quench oscillator causes repeated build up and decay of oscillations and the oscillations are maximum at the zero crossing where the quench signal goes towards the positive half cycle. Any phase errors in the quench signal directly affects the phase detection performance. Thus it is also important to maintain synchronization between the quench signal and the carrier.
In digital communications, packet arrival instants are generally random and unknown at the receiver. The payload of the packet can be successfully demodulated if the start time of the payload is known at the receiver.
Thus the objective of this thesis is threefold. Firstly the super regenerative architecture for demodulating BPSK signals is presented and an analyses based on performance and power is done. Secondly a method for synchronizing the quench signal to the carrier is presented and the effects of jitter on the detection performance is analysed. Thirdly, the procedure for preamble detection is presented and its performance is analysed.

Table of Contents

List of Figures

List of Tables

Acknowledgements

First and foremost, I would like to thank Dr. Guido Dolmans and my supervisor Dr. Li Huang for providing me the opportunity to work at IMEC, Holst Centre. I would like to convey special thanks to Li for his valuable guidance and advice without which the project would not have been possible. Thank you very much Li.
I take immense pleasure in thanking my colleagues at IMEC for being a constant source of encouragement. Special thanks to Dr. Nauman F.Kiyani who was always available to me in-spite of his busy schedule, providing me valuable technical suggestions which greatly helped me in this project. Thanks a lot Nauman. I am highly indebted to my supervisor Prof. Gerard Janssen for his guidance and constant supervision and for providing necessary information regarding the project. Under your guidance I have experienced "never give up" attitude in facing each difficulty with confidence. Thank you very much for your support sir. I would also like to thank my friends Venkat, Ananth, Gijs and Praveen for being a constant source of inspiration throughout this project. I would thank my parents for their unceasing support, both financially and emotionally throughout this degree program.
I thank the Almighty for the wisdom and perseverance bestowed upon me during this project and indeed, throughout my life.

Delft
July 9, 2012

Deepak Shastry Ravishankar

Chapter 1

Introduction

1-1 Introduction to Radio Receivers

In digital radio communications, a radio receiver is an electronic device that receives radio waves and extracts the desired information carried by the radio waves. The receiver uses filters to separate the wanted radio frequency signal from other signals, also an electronic amplifier is used to increase the power of the signal for further processing, and finally recovers the desired information through demodulation. The world's first radio receiver known as "thunderstorm register" was designed by Alexander Stepanovich Popov in 1896 [3]. In 1916 Lee de forest invented vacuum tubes, a that relatively amplifies weak electrical signals. At the same time Tuned Radio Frequency Receiver (TRF) was invented by Ernst Alexanderson showed major improvement in performance over other receivers that was available before, but the inherent working of the TRF, where all the tuned stages of the radio must track and tune to the desired reception frequency made the receiver cumbersome and a power hungry device [3].

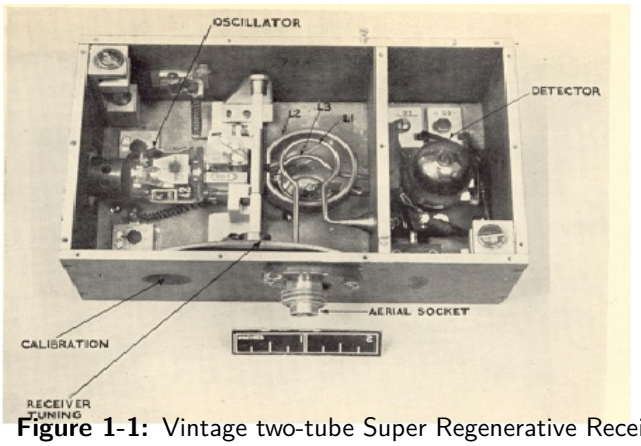

Figure 1-1: Vintage two-tube Super Regenerative Receiver

In 1920, an American inventor Edwin Howard Armstrong invented and patented Super Regenerative (SR) Receiver [4]. Super regenerative receiver required fewer components than other types of receiver circuit used during that time. The main attraction of the SR receiver is that it provides more amplification out of the expensive vacuum tubes requiring fewer stages of amplification in contrast to TRF receivers. The TRF receivers often required 5 or 6 vaccum tubes, each stage requiring tuned circuits, making the receiver more bulky and power hungry. Figure 1-1 shows a vintage two-tube Super Regenerative Receiver [5]. This receiver consists of a SRO, an input coupling transformer, a tunable capacitor, and a detector tube. Manual adjustments are necessary to tune the oscillator frequency and loop gain. In 1930 the SR receiver was replaced by the superheterodyne circuit due to its superior performance [4]. In recent years the SR receivers has seen a modest comeback in receiver design. The reasons for its success is that the SR receiver included a minimal number of required active devices, a high RF gain, and the ability to operate at high RF frequencies. It finds major applications in garage door openers, key-less locks, RFID readers etcetera to name a few.

1-2 Problem Formulation

SR circuit was primarily intended to be used as a narrow band AM receiver. Despite many years of development, they still suffer from poor selectivity and lack of stability, while having the potential to be used for low power applications. In the classical super regenerative receivers, the RF oscillations obtained at the output of the oscillator are applied to a non linear detector followed by a low pass filter. Therefore the demodulation capabilities of the SR architecture is limited to demodulate OOK signals only. The main challenge is to use the super regenerative architecture to demodulate phase modulated signals which are more robust to interference compared to OOK signals and still maintaining the low power, low cost features of the receiver. In this thesis an attempt is made to address this research gap.
The main goal of this project is to provide mathematical models for implementing a modified SR receiver architecture for the demodulation of BPSK and DPSK signals. Furthermore, the issues like quench synchronization, effects of phase jitter in the SR receiver and frame synchronization techniques are addressed and incorporated in this model.

1-3 Thesis Highlights

In chapter (2), the general principle of the super regenerative receiver is explained, a signal model for super regenerative receiver is described and mathematical analysis for super regenerative receiver in the presence of AWGN is performed. In chapter (3), two different super regenerative receiver architectures are described which can be used to demodulate binary phase shift keying(BPSK) and differential phase shift keying (DPSK) signals. The two architectures are compared based on performance and power consumption. In chapter (4), a system model is provided which explains the

synchronization process using a phase locked loop, also a mathematical analysis is done to obtain the relation between the phase/timing jitter and the detection performance. In chapter (5), an algorithm is proposed which describes the procedure for preamble detection. The performance of signal detection obtained is analysed by using probability of detection and error probabilities like probability of miss detection and probability of false alarm.

Chapter 2

Introduction to Super Regenerative Receivers

The Super Regenerative(SR) circuits were mainly used as narrow band AM receivers since its invention in the 1922. Today the SR circuit architecture finds its application in the design of direct sequence spread spectrum receivers [6], demodulation of phase and frequency modulated signals [7] and reception of ultra wideband impulse radio modulations [8]. The reasons for its success are due to the simplicity of the design, low cost, high gain, high efficiency, low power and its ability to operate at high Radio Frequencies (RF). These features enabled an attractive architecture for low power wireless receivers [9]. The commercial applications for SR receivers are many, to name a few are: sensor networks, short distance telemetry, home automation, biomedicine, remotely controlled systems. In this chapter, the operation of the super-regenerative receiver is introduced on a system level and a mathematical model of the super regenerative receiver in the presence of AWGN is analysed.

2-1 Super Regenerative Receiver Signal model

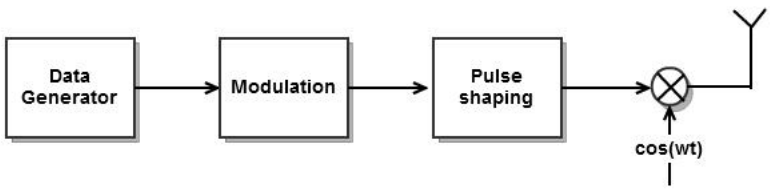

Figure 2-1: Block Diagram of the transmitter

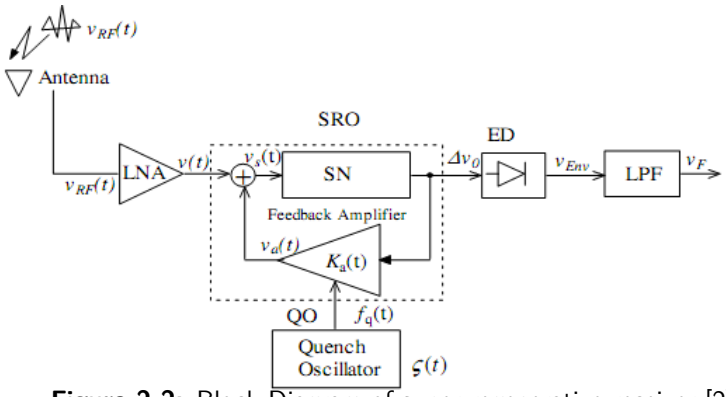

Figure 2-2: Block Diagram of super regenerative receiver [2]

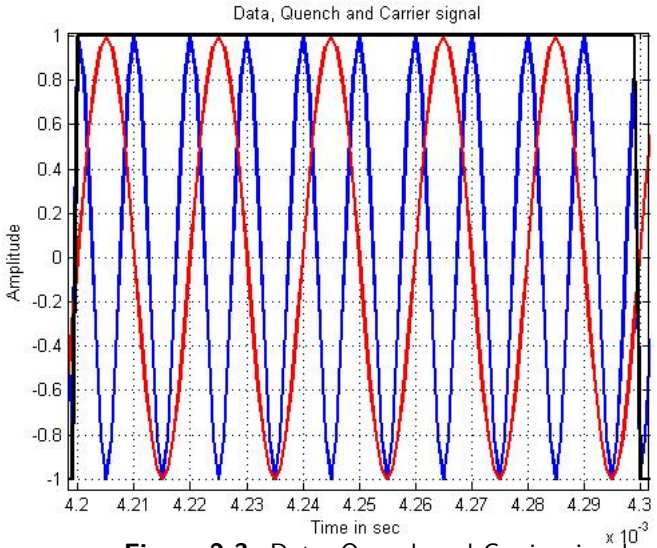

Figure 2-3: Data, Quench and Carrier signal

The block diagram is shown in the figures 2-1 and 2-2. It consists of a transmitter part and a receiver part. The transmitter part consists of a Data Generator, BPSK Modulator, Pulse Shaper and a locally generated carrier signal. The receiver part is a classical Super Regenerative Receiver which comprises of a super regenerative oscillator which is modelled as a frequency selective network with a feedback loop along with a variable gain amplifier. A quench oscillator controls the gain of the super regenerative oscillator. The quench oscillator is followed by an envelope detector and a low pass filter.

The Data generator block generates a stream of binary information bits and the BPSK modulator maps these information bits to signal waveforms. In other words if the information sequence is transmitted 1 bit at a time at a uniform rate of R_b bits per second, then BPSK modulator transmits 1 information bit at a time at the rate of R_b bits/s by using M = 2^1 distinct waveforms say $x_i(t)$, where i = 0,1,... M-1. The signal received at the input of the super regenerative receiver can be written as

$$v_{rf}(t) = x(t) + n(t) \tag{2-1}$$

$$x(t) = Vp_c(t)cos(\omega t + \phi_i) \tag{2-2}$$

where V is the peak amplitude, $p_c(t)$ is the normalized envelope of the input pulse shape, ϕ_i denotes the BPSK phase information which can take values of $\phi_i = 0$ or π, $n(t)$ is the Additive White Gaussian Noise with power spectral density $\frac{N_o}{2}$, $\omega = 2\pi f_c$ is the locally generated carrier frequency.
The main principle of the super regenerative receiver is that the quench oscillator causes a periodic build up and decay of RF oscillations. Therefore, the signal coming out of the super regenerative oscillator consists of RF pulses separated by a quench period T_q. The equation for the quench signal can be written as [10]

$$v_q(t) = \zeta_o sin(2\pi f_q t + \phi_q) \tag{2-3}$$

where f_q is the quench frequency, ζ_o is the maximum amplitude of the quench signal. In this model the carrier frequency f_c, quench frequency f_q and the transmit bit rate R_b holds the following relation

$$f_c = mR_b \tag{2-4}$$
$$f_c = nf_q \tag{2-5}$$
$$f_q = qR_b \tag{2-6}$$
$$\therefore x(t) = Vp_c(t)cos(2\pi mR_b t + \phi_i) \tag{2-7}$$
$$v_q(t) = \zeta_o sin(2\pi qR_b t + \phi_q) \tag{2-8}$$

where m, n, q are positive integers (m = n = q = 1, 2, 3, ...). This is also shown in figure 2-3, where the black coloured signal is the data sequence transmitted at the rate of $R_b = 10KHz$. The red coloured signal is the quench signal with frequency $f_q = 40KHz$ and the blue coloured signal is the carrier signal with frequency $f_c = 100KHz$.
Super regenerative receiver operates in 2 modes: the linear mode and the logarithmic mode. In the linear mode the super regenerative oscillator does not reach equilibrium during the quench period, the amplitude of the RF oscillations are measured before they reach equilibrium. In the logarithmic mode, the oscillations are allowed to reach its maximum value during each quench cycle and the detection is based on calculating the energy of the oscillations [10].
As explained in [10], the role of the quench signal in the super regenerative receiver is very important to understand the operation of the receiver. The quench oscillator basically controls the gain of the super regenerative oscillator. It generates a quenching signal which consists of periodic quench cycles. Figure 2-4 shows the RF input signal, Quench signal and the SRO output.
During the start of a new quench cycle, as shown in figure 2-4, the quench signal goes towards the positive half cycle where the presence of any oscillations in the super regenerative oscillator are damped. When the quench signal returns to 0 and moves towards the negative half cycle, the oscillation builds up from the injected signal and it becomes maximum when the quench signal returns back to 0 at the end of the quench cycle. In this way, the quench oscillator causes repeated build up and decay of RF pulses and thus the output of the SRO comprises of RF pulses separated by the quench period [10]. The RF oscillations obtained at the output of the oscillator are applied to a non linear detector followed by a low pass filter. Hence the demodulation capabilities of super regenerative receiver was restricted to amplitude modulated signals only.

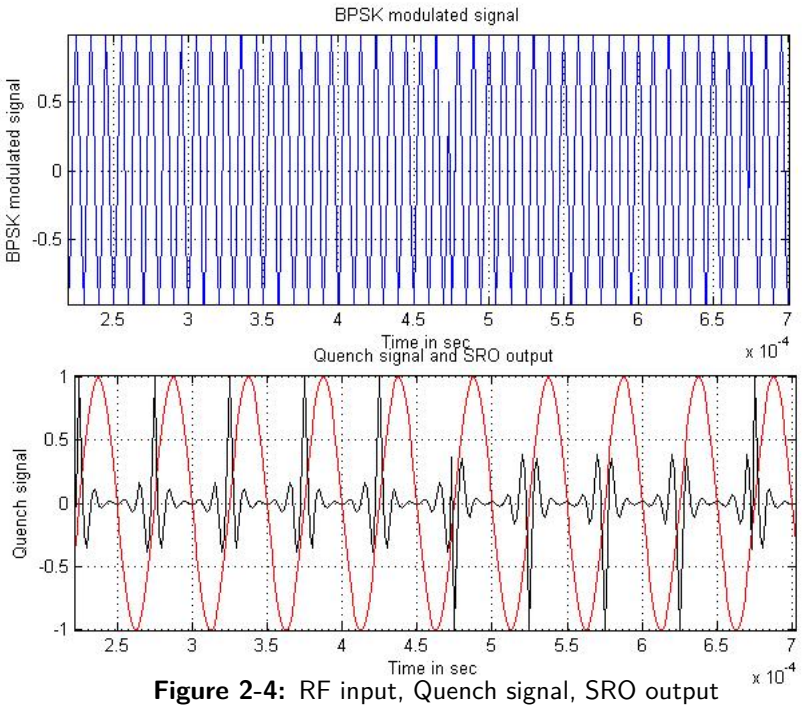

Figure 2-4: RF input, Quench signal, SRO output

2-2 Design Analysis of a Super Regenerative Receiver in the presence of Noise

The Selective Network (SN) shown in figure 2-2 can be characterised by using a differential equation as given in [10]. When the super regenerative receiver is operated in linear mode, the output voltage of the super regenerative oscillator is obtained by solving this differential equation as explained in [10].
In the presence of a BPSK signal embedded in noise (2-9), the expression for the received signal at the output of the super regenerative oscillator can be written as shown in (2-10)

$$v_{in}(t) = V p_c(t) \cos(\omega t + \phi_i) + n(t) \tag{2-9}$$

$$v_{out}(t) = v_{signal}(t) + v_{noise}(t) \tag{2-10}$$

where V is the peak amplitude, $p_c(t)$ is the normalized envelope of the input pulse shape, ϕ_i denotes the BPSK phase information which can take values of $\phi_i = 0$ or π. The output signal $v_{out}(t)$ given in (2-10) contains two components: signal component $v_{signal}(t)$ and the noise component $v_{noise}(t)$. The signal and the noise components can be written as

$$v_{signal}(t) = V\zeta_o K_o K_s p(t) \int_{t_a}^{t_b} p_c(\tau) s(\tau) \cos((\omega - \omega_o)\tau + \omega_o t + \phi_i)\, \mathrm{d}\tau. \tag{2-11}$$

$$v_{noise}(t) = 2\zeta_o \omega_o K_o K_s p(t) \int_{t_a}^{t_b} n(\tau) s(\tau) \sin(\omega_o(t - \tau))\, \mathrm{d}\tau. \tag{2-12}$$

where $s(t)$ is the super regenerative receiver's sensitivity curve and it should not be confused with minimum magnitude of the input signal, $p(t)$ is the normalized envelope generated at the output of the super regenerative oscillator, K_o, K_s contribute to super regenerative gain, ζ_o gives the maximum amplitude of the quench signal, $n(t)$ is the Additive White Gaussian Noise with power spectral density $\frac{N_o}{2}$, t_a and t_b represent the start and end time intervals in seconds of a single quench cycle.
Assuming that the transmitter frequency is tuned to the receiver frequency i.e. $\omega = \omega_o$, we can write (2-11) as

$$v_{signal}(t) = V\zeta_o K_o K_s p(t) \int_{t_a}^{t_b} p_c(\tau)s(\tau)\cos(\omega_o t + \phi_i)\,\mathrm{d}\tau. \tag{2-13}$$

The probability density function of received signal at the output of the super regenerative oscillator can be derived based on the following. If X is a random variable defined as $X \sim \mathcal{N}(\mu, \sigma^2)$ and if another random variable Y is defined as $Y = \sum_i a_i X + b$ then the PDF of Y results in Gaussian Distribution with mean and variance given as

$$\mu_Y = \sum_i a_i \mu_i + b \tag{2-14}$$

$$\sigma_Y^2 = \sum_i a_i^2 \sigma^2 \tag{2-15}$$

When the super regenerative receiver is operated in linear mode, the received signal at the output of SRO is a result of linear operations on Gaussian distributed signal and this too has a gaussian distribution with mean and variance as calculated below.
Using (2-13),(2-12) and (2-15) the noise variance can be calculated as

$$\sigma_{SRO}^2 = A^2\sigma^2 \int_{t_a}^{t_b} s^2(\tau)\sin^2(\omega_o(t-\tau))\,\mathrm{d}\tau. \tag{2-16}$$

where $A = 2\zeta_o\omega_o K_o K_s p(t)$ is a constant that contributes to the noise amplitude, σ^2 is the variance of $n(\tau)$ given in (2-12). Expanding the sine term in (2-16) we can write

$$\sigma_{SRO}^2 = \frac{A^2\sigma^2}{2} \int_{t_a}^{t_b} s^2(\tau)(1-\cos(2\omega_o(t-\tau))\,\mathrm{d}\tau. \tag{2-17}$$

Neglecting the higher frequency term in (2-17) we get

$$\sigma_{SRO}^2 = \frac{A^2\sigma^2}{2} \int_{t_a}^{t_b} s^2(\tau)\,\mathrm{d}\tau. \tag{2-18}$$

Substituting for σ^2 and A in (2-18) and simplifying we get

$$\sigma_{SRO}^2 = (\zeta_o\omega_o K_o K_s p(t))^2 N_o \int_{t_a}^{t_b} s^2(\tau)\,\mathrm{d}\tau. \tag{2-19}$$

Therefore the resulting noise component has a gaussian distribution with zero mean and variance given by σ_{SRO}^2. The mean of the received signal is given by the maximum amplification of the received signal in the absence of noise and this is given by

$$\mu_{SRO} = max(v_{signal}(t)). \tag{2-20}$$

Hence the probability density function of the received signal at the output of super regenerative receiver can be written as

$$p(x) = \frac{1}{\sqrt{2\pi\sigma_{SRO}^2}} e^{\frac{-(x-\mu_{SRO})^2}{2\sigma_{SRO}^2}} \tag{2-21}$$

In general the average power of a signal $v_{signal}(t)$ at any given time interval T can be written as

$$P_{v_{signal}} = \frac{1}{T}\int_0^T v_{signal}^2(t)\,\mathrm{d}t \tag{2-22}$$

Using (2-22), the signal power of (2-13) can be obtained as

$$P_{v_{signal}} = \frac{1}{T}\int_0^T B^2\left(\int_{t_a}^{t_b} p_c(\tau)s(\tau)\,\mathrm{d}\tau\right)^2 \cos^2(\omega_o t + \phi_i)\,\mathrm{d}t \tag{2-23}$$

where $B = V\zeta_o K_o K_s p(t)$ which contributes to signal amplification. Expanding the cos term in (2-23)we get

$$P_{v_{signal}} = \frac{1}{2T}\int_0^T B^2\left(\int_{t_a}^{t_b} p_c(\tau)s(\tau)\,\mathrm{d}\tau\right)^2 \mathrm{d}t + \frac{1}{2T}\int_0^T B^2\left(\int_{t_a}^{t_b} p_c(\tau)s(\tau)\,\mathrm{d}\tau\right)^2 \cos(2(\omega_o t + \phi_i))\,\mathrm{d}t \tag{2-24}$$

Neglecting the high frequency term in equation (2-24) the average signal power can be written as

$$P_{v_{signal}} = \frac{1}{2T}\int_0^T B^2\left(\int_{t_a}^{t_b} p_c(\tau)s(\tau)\,\mathrm{d}\tau\right)^2 \mathrm{d}t \tag{2-25}$$

Simplifying further we get

$$P_{v_{signal}} = \frac{B^2}{2}\left(\int_{t_a}^{t_b} p_c(\tau)s(\tau)\,\mathrm{d}\tau\right)^2 \tag{2-26}$$

Hence we can write the Signal to Noise Ratio at the output of the super regenerative oscillator as

$$SNR_{out} = \frac{V^2(\int_{t_a}^{t_b} p_c(\tau)s(\tau)\,\mathrm{d}\tau)^2}{2N_o\int_{t_a}^{t_b} s^2(\tau)\,\mathrm{d}\tau} \tag{2-27}$$

The signal to noise ratio at the output of the super regenerative oscillator can be expressed in terms of E_b/N_o and can be written as [2]

$$SNR_{out} = \frac{E_b}{N_o}\frac{(\int_{t_a}^{t_b} p_c(\tau)s(\tau)\,\mathrm{d}\tau)^2}{\int_{t_a}^{t_b} p_c^2(\tau)\,\mathrm{d}\tau\int_{t_a}^{t_b} s^2(\tau)\,\mathrm{d}\tau} \tag{2-28}$$

where,

$$E_b = \frac{V^2}{2} \int_{t_a}^{t_b} p_c^2(\tau)\, \mathrm{d}\tau \tag{2-29}$$

$$\frac{(\int_{t_a}^{t_b} p_c(\tau) s(\tau)\, \mathrm{d}\tau)^2}{\int_{t_a}^{t_b} p_c^2(\tau)\, \mathrm{d}\tau \int_{t_a}^{t_b} s^2(\tau)\, \mathrm{d}\tau} \leq 1. \tag{2-30}$$

An optimum value of SNR_{out} can be obtained when $p_c(t) = s(t)$. Therefore using Schwarz's inequality, the fractional part in (2-29) will be equal to one. Hence

$$SNR_{out} = \frac{E_b}{N_o} \quad \text{for } p_c(t) = s(t). \tag{2-31}$$

2-3 Summary

In this chapter, the operation of super regenerative receiver on a system level is introduced. A mathematical analysis of the super regenerative receiver in the presence of AWGN channel is discussed, where the expressions for the probability density function and the signal to noise ratio at the output of super regenerative receiver were derived and the condition for optimum signal to noise ratio is obtained.

Chapter 3

BPSK Based Super Regenerative Receiver Architectures

3-1 Introduction

In the classical super regenerative receiver, the RF oscillations obtained at the output of the oscillator are applied to a non linear detector followed by low pass filter. Hence the demodulation capabilities of super regenerative receivers were restricted to amplitude modulated signals. Here we modify the architecture of the super regenerative receiver which can be used to demodulate PSK signals. There are very few techniques provided in the literature where the super regenerative receiver is used to demodulate PSK signals. [7] explains one such technique where the super regenerative oscillator is used along with a transmission line which supports two modes of oscillations depending on a control signal. In the first mode, the signal that is generated has no dc component and is an exponentially growing oscillation whose phase is coherent with the phase of the received signal. At a given instant, the circuit topology is switched to generate the second mode of oscillation which is characterized by producing a waveform consisting in the sum of a) a similar waveform whose frequency is twice the frequency of the first mode and b) an exponentially growing low frequency component whose amplitude is proportional to the cosine of the generated signal phase in the first topology at the moment of switching. The signal that is generated is low-pass filtered which results in retrieving a dc component whose sign is used to decide the received bit in a BPSK modulation.
[11] provides another technique where the classical super regenerative oscillator generates the RF pulses where the regenerative receiver preserves the phase information. Once the generated signal achieves sufficient amplitude, the signal at the output of the SRO is sampled by a conventional D flip-flop which, at the same time, decides the received bit.
In this chapter two different super regenerative architectures are described which can

be used to demodulate BPSK and DPSK signals. The presented architectures are compared based on their performance and power consumption.

3-2 Differential BPSK to OOK conversion

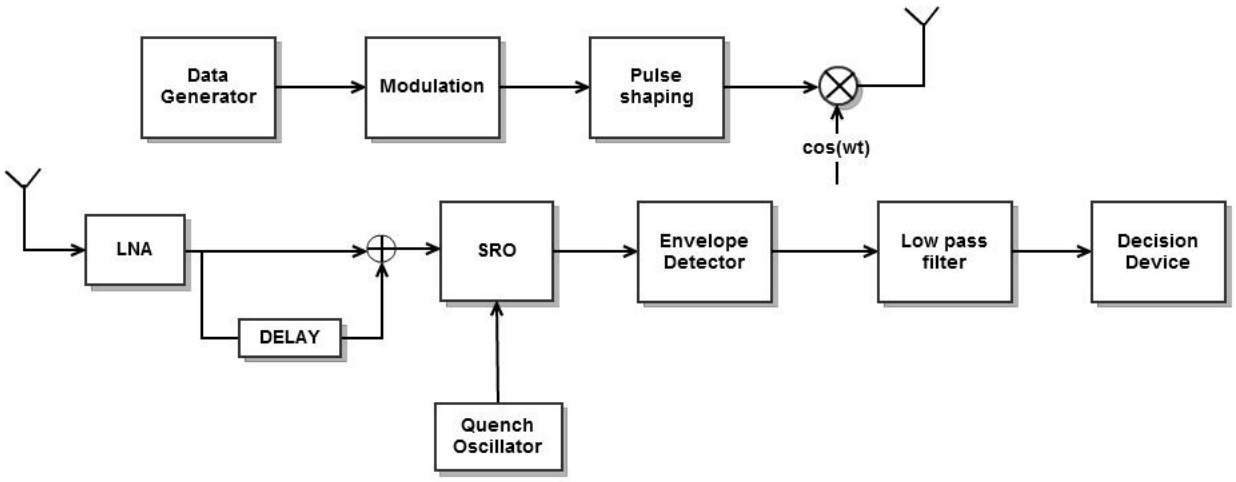

Figure 3-1: Block Diagram of super regenerative receiver with PSK to OOK conversion

In this architecture a Differential BPSK signal is transformed into an OOK signal using a delay circuit and an adder as shown in figure 3-1. A conventional Super Regenerative Receiver architecture can then be used to detect the OOK symbols. In this scenario we consider the delay line with a delay of 1 symbol period T_s and the symbol period is assumed to be an integer multiple of carrier period [12]. A DPSK modulated signal embedded in noise can be written as

$$v(t) = V * cos(\omega_o t + \phi_1) + n(t) \tag{3-1}$$

where ϕ_1 is the phase information of the signal, V is the amplitude of the input signal and $n(t)$ is zero mean Additive White Gaussian Noise with variance σ^2. When the received signal is passed through a delay circuit it results in a time shifted version of the signal which can be represented as $v(t-\tau)$ and this time shift also results in a phase shift of the received signal. Let us represent the phase of the shifted signal as ϕ_2. When the received signal is added with its time shifted version resulting in an ASK modulated signal. This is derived as follows.
If the resultant signal at the output of the delay and adder circuit be represented as

$v_o(t)$ then

$$v_o(t) = V[\cos(\omega_o t + \phi_1) + \cos(\omega_o(t-\tau) + \phi_1)] + n(t) + n(t-\tau)] \quad (3\text{-}2)$$
$$= V[\cos(\omega_o t + \phi_1) + \cos(\omega_o t + \phi_2)] + n(t) + n(t-\tau)] \quad (3\text{-}3)$$

where $\phi_2 = \phi_1$ - $\omega_o\tau$. Simplifying (3-3) we get

$$v_o(t) = 2 * V\left[\cos\left(\frac{2\omega_o t + \phi_1 + \phi_2}{2}\right)\cos\left(\frac{\phi_1 - \phi_2}{2}\right)\right] + n(t) + n(t-\tau) \quad (3\text{-}4)$$

Simplifying further

$$v_o(t) = 2 * V\left[\cos\left(\omega_o t + \frac{\phi_1 + \phi_2}{2}\right)\cos\left(\frac{\phi_1 - \phi_2}{2}\right)\right] + n(t) + n(t-\tau) \quad (3\text{-}5)$$

Simplifying this further we get

$$v_o(t) = 2 * V\left[\cos\left(\omega_o t + \frac{\phi_1 + \phi_2}{2}\right)\cos\left(\frac{\phi_1 - \phi_2}{2}\right)\right] + n(t) + n(t-\tau) \quad (3\text{-}6)$$

Therefore we can write

$$v_o(t) = \begin{cases} 2 * V\cos\left(\omega_o t + \phi_1\right) & \text{if } \phi_1 = \phi_2, \\ n(t) + n(t-\tau) & \text{if } \phi_1 = 0 \text{ and } \phi_2 = \pi. \end{cases} \quad (3\text{-}7)$$

3-2-1 Example of DBPSK converting to OOK

Let the transmitted sequence be 1 1 0 1 0 as shown in table 3-1. At first the transmitted sequence is modulated using DPSK modulation and then delayed by symbol time. The resulting two signals are added to get a ASK signal. The steps are explained below:

- Let symbol 1 of the transmitted sequence is coded as “keep previous phase”, while symbol 0 is coded as “change previous phase”.
- Let $+V$ be an RF pulse having amplitude V and positive phase and $-V$ be an RF pulse having amplitude V and negative phase.
- Whenever the transmitted symbol is 1 the previous phase is retained and when the transmitted symbol is 0 then there is phase change of π radians w.r.t to previous phase, the resulting sequence is a DPSK modulated sequence shown in the table 3-1.
- The DPSK signal is shifted by the symbol period and the resulting “Shifted Sequence” is shown in the table 3-1
- The two sequences are added together to get an OOK signal. There will be double amplitude for symbol 1 and zero amplitude for symbol 0 (i.e., just like ASK modulation, note that the envelope detector will remove negative sign).

Table 3-1: Converting DBPSK to OOK

Tx Sequence		1	1	0	1	0
Pulse Sequence	+V(initial bit)	+V	+V	-V	-V	+V
Shifted Sequence		+V	+V	+V	-V	-V
Sum		+2V	+2V	0	-2V	0

3-2-2 Probability Density at the output of the Super Regenerative Oscillator

In the linear mode, the signal at the output of the super regenerative oscillator is passed through an envelope detector. When a symbol 1 is transmitted, the output signal is Rician distributed [13]. If $v_{env}(t)$ is used to represent the voltage at the output of the envelope detector, then

$$p(v_{env} \mid s_i = 1) = \frac{v_{env}}{\sigma^2_{SRO}} e^{-\frac{v^2_{env}+B^2}{2\sigma^2_{SRO}}} I_o\left(\frac{v_{env}B}{\sigma^2_{SRO}}\right) \tag{3-8}$$

where B is the maximum amplitude of the received signal as given in (2-23). If the mean and variance of v_{env} can be denoted as μ_{rician} and σ^2_{rician} respectively then [13]

$$\mu_{rician} = \sigma\sqrt{\frac{\pi}{2}} L_{\frac{1}{2}}\left(\frac{-B^2}{\sigma^2_{SRO}}\right) \tag{3-9}$$

$$\sigma^2_{rician} = 2\sigma^2_{SRO} + B^2 - \frac{\pi\sigma^2_{SRO}}{2} L^2_{\frac{1}{2}}\left(\frac{-B^2}{\sigma^2_{SRO}}\right) \tag{3-10}$$

where $L_q(x)$ denotes a Laguerre polynomial. When symbol 0 is transmitted, the incoming signal can be modelled as AWGN, also since the received signal at the output of the SRO is Gaussian, the envelope of a Gaussian distributed random variable results in a Rayleigh distribution [13]. The PDF of which is given by

$$p(v_{env} \mid s_i = 0) = \frac{v_{env}}{\sigma^2_{SRO}} e^{-\frac{v^2_{env}}{2\sigma^2_{SRO}}} \tag{3-11}$$

having mean and variance is given by $\mu_{ray} = \sigma_{SRO}\frac{\pi}{2}$ and $\sigma_{ray} = \frac{4-\pi}{2}$ respectively. The decision whether a symbol is transmitted can be made based by comparing $v_{env}(t)$ against some threshold. If β denotes the threshold level, then the received symbol is 1 if $v_{env}(t) \geq \beta$ and 0 if $v_{env}(t) < \beta$. The probability of error when symbol 1 was transmitted is [14]

$$\begin{aligned} P_{e1} = Prob(v_{env} \leq \beta) &= \int_0^{\beta} p(v_{env} \mid s_i = 1)\, \mathrm{d}v_{env} \\ &= 1 - \int_{\beta}^{\infty} p(v_{env} \mid s_i = 1)\, \mathrm{d}v_{env} \\ &= 1 - \int_{\beta}^{\infty} \frac{v_{env}}{\sigma^2_{SRO}} e^{-\frac{v^2_{env}+B^2}{2\sigma_{SRO}}} I_o\left(\frac{v_{env}B}{\sigma^2_{SRO}}\right) \end{aligned} \tag{3-12}$$

(3-12) can be simplified by applying the following transformations

$$r^2 = \frac{v_{env}^2}{\sigma_{SRO}^2} \tag{3-13}$$

$$\rho = \frac{B^2}{2\sigma_{SRO}^2} \tag{3-14}$$

$$b_o = \frac{\beta}{\sigma_{SRO}} \tag{3-15}$$

$$\tag{3-16}$$

on substituting we get

$$\begin{aligned} P_{e1} &= 1 - \int_{b_o}^{\infty} r e^{-\frac{r^2+\sqrt{2\rho}}{2}} I_o\left(\frac{r\sqrt{2\rho}}{\sigma_{SRO}^2}\right) \\ &= 1 - Q(\sqrt{2\rho}, b_o) \end{aligned} \tag{3-17}$$

where $Q(a,b) = \int_b^{\infty} \exp(-\frac{a^2+x^2}{2}) I_o(ax) x \, \mathrm{d}x$ is called the marcum Q function, $b_o = \frac{\beta}{\sigma_{SRO}^2}$is the threshold level normalized to rms noise and $\rho = \frac{B^2}{2\sigma_{SRO}^2}$ is the signal to noise ratio at the SRO output. The probability of error when 0 was transmi tted is

$$\begin{aligned} P_{e0} = Prob(v_{env} > \beta) &= \int_{\beta}^{\infty} p(v_{env} \mid s_i = 0) \, \mathrm{d}v_{env} \\ &= exp\left(-\frac{b_o^2}{2}\right) \end{aligned} \tag{3-18}$$

Assuming that the symbols 1's and 0's are transmitted with equal probability, the average probability of error is given by

$$P_e = \frac{1}{2}(1 - Q(\sqrt{2\gamma}, b_o)) + \frac{1}{2} exp(-\frac{b_o^2}{2}) \tag{3-19}$$

The optimal threshold can be derived by calculating the value of b_o which minimizes the probability of error given in (3-19) for each SNR. The probability of error can be minimized by partially differentiating (3-19) w.r.t b_o and equating the result to 0 i.e.,$\frac{\partial P_e}{\partial b_o} = 0$. The result of this operation yields the following equation [14]

$$exp(-\gamma) I_o(b_o\sqrt{2\gamma}) = 1 \tag{3-20}$$

and the solution of 3-20 yields b_o

$$b_o = \sqrt{2 + \frac{\gamma}{2}} \tag{3-21}$$

Figure 3-2 shows the DPSK Bit Error Rate comparison of an optimum receiver and the Super Regenerative Receiver. We can observe a degradation of about 2 db with Super Regenerative Receiver. From the figure we can see that this degradation is due to the fact the SRO only outputs samples at the end of every quench period and the whole signal energy is not utilized for detection.

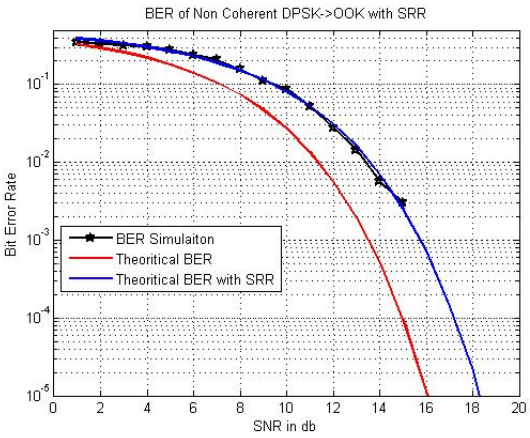

Figure 3-2: DBPSK bit error rate comparison

3-3 BPSK based Super Regenerative Receiver

Here we present a super regenerative architecture which can be used for BPSK demodulation without converting the input signals from PSK to OOK. The system model of the proposed architecture is shown in figure 3-3. It comprises of a transmitter part and a receiver part. The transmitter part contains a Data generator, BPSK Modulator and a Pulse Shaping device. The receiver part consists of a Super Regenerative Oscillator, Quench Oscillator which controls the gain of the SRO, Analog to Digital Converter, Phase Detector and a Decision Device.

The received signal at the output of the super regenerative oscillator is passed through ADC, where the received signals are sampled at quench rate, the resulting signal is then passed through detection stage where the BPSK signals are detected.

3-3-1 BPSK Demodulation

The signal at output of Super Regenerative Oscillator follows the equation (2-10) explained in section 2-2 in chapter 2 . This signal is sampled by the ADC, the phase of the resulting signal is calculated by comparing the amplitudes to a threshold 0. If the received sample has an amplitude greater than 0 then the phase is taken as zero else the phase is taken as π. The SRO always preserves the input phase [11] and as explained in the signal model in section 2-1, we obtain q number of phases per symbol period. The symbols can be detected by averaging the phases obtained per symbol period and comparing it with a threshold phase ($\phi_{threshold} = \pm\ \pi/2$), this is explained below.

Step 1: Find the average phases of the received symbols.
Let

$$\phi_{A,q_i} = [\phi_{A,q_1} \dots \phi_{A,q_q}]^T \tag{3-22}$$

be the phases obtained for each symbol $A = -1, 1$. If ϕ_{avg_A} is the mean phase obtained for symbols -1 and 1 by averaging (3-22) then the decision is made on the following

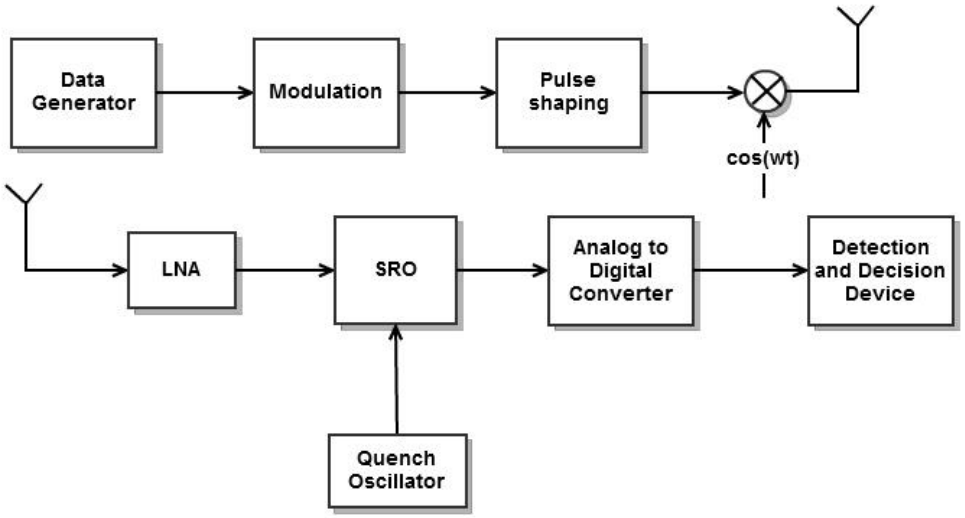

Figure 3-3: Block diagram of BPSK based super regenerative receiver

condition
Step 2: Detection.

$$S_i = \begin{cases} 0 & \text{if } \phi_{avg_A} \leq \phi_{threshold}, \\ 1 & \text{if } \phi_{avg_A} > \phi_{threshold}. \end{cases} \tag{3-23}$$

3-3-2 Differential PSK Demodulation

In DPSK modulation, the input bit sequence is encoded such that the information is present in the phase difference between two successive symbols rather than phase itself. The DPSK signal $r_i(t)$ and the phase encoding process is given by

$$r_i(t) = Vp_c(t)cos(2\pi f_c t + \phi_i) \tag{3-24}$$

where $p_c(t)$ is the input pulse shape, ϕ_i is the phase of the i^{th} bit. The phase encoding rule is explained below.

$$\phi_i = \begin{cases} \phi_{i-1} & \text{if } d_i = 1, \\ \phi_{i-1} + \pi & \text{if } d_i = 0. \end{cases} \tag{3-25}$$

where $d_i \in \{0, 1\}$. Let us assume that bit 1 is coded as "keep previous phase", while bit 0 is coded as "change previous phase". Whenever the transmitted symbol is 1, the previous phase is retained and when the transmitted symbol is 0 then there is a phase

Table 3-2: Differential Encoding

Tx Sequence		1	1	0	1	0
Pulse Sequence	+A(initial bit)	+A	+A	-A	-A	+A

change of π radians w.r.t to the previous phase. This is shown in table 3-2.
A DBPSK modulated signal embedded in noise when passed through the SRO, results in similar equations for Signal to Noise Ratio as explained in section (2-2). However the detection technique will be different compared to BPSK detection. As explained in section (3-3-1) we obtain q phases per symbol due to the sampling process at the end of every quench cycle. The average phase for each symbol is obtained by averaging all q phases per symbol. If a vector $\phi^d = [\phi_1^d \dots \phi_N^d]$ denotes the average phases of the N samples in received signal then symbol detection is made based on the following condition

$$S_i = \begin{cases} 0 & \text{if } \phi_i^d - \phi_{i-1}^d \geq \frac{\pi}{2} \ \ \& \ \ \phi_i^d - \phi_{i-1}^d < \frac{3\pi}{2}, \\ 1 & \text{otherwise} \end{cases} \tag{3-26}$$

Figure 3-4 shows the bit error rate comparison of demodulation of BPSK and DBPSK

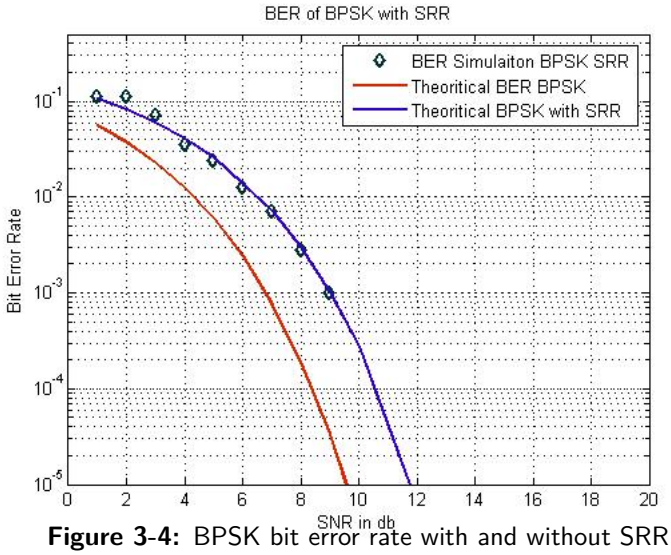

Figure 3-4: BPSK bit error rate with and without SRR

modulated signals in the presence and absence of Super Regenerative Receivers. From the figure it is noted that Super Regenerated Receiver degrades the performance approximately around 2 db.

Table 3-3: Power breakup in milli watts for architecture presented in section 3-3

Block	2.4GHz	1GHz
LNA	0.490	0.240
SRO	0.216	0.396
ADC	0.1	0.1
Quench oscillator	0.28	0.300
Total Power	1.08	1.03

3-4 Power analysis

The main reason for considering super regenerative receiver is due to its simplicity, low power consumption and low cost. Let us compare the two architectures presented in sections (3-2) and (3-3) respectively for its power consumption. This thesis does not discuss ultra low power implementation aspects of the presented architectures, however with the recent work carried out in literature on the implementation of the SR receiver, an attempt is made to perform the power consumption analysis for the presented architectures.
For convenience let us denote the architecture presented in section (3-2) as architecture 1 and the one presented in section (3-3) as architecture 2. The analog components present in architecture 2 contain an LNA, super regenerative oscillator, Quench Oscillator and ADC. The receiver blocks in figure 3-3 are connected in cascade and the power consumption for each block can be calculated using the power formula given in [15].
Table 3-3 gives the measured power consumed by each analog block in the super regenerative receiver for a data rate of 1 Mbps and 100 Kbps and operating frequency of 2.4 GHz and 1 GHz respectively for architecture 2. The power consumed by LNA, super regenerative block, Quench Oscillator is taken from experimental results conducted in [16] for 2.45 GHz and [17] for 1 GHz respectively. The power consumed by ADC is taken from experimental results conducted in [18]. These power values are measured for the receiver specifications given in appendix (A).
Coming to architecture 1, as explained in section (3-2), the delay line of one symbol period T_s is considered and the symbol period is assumed to be an integer multiple of carrier period. So for a data rate of 1 Mbps (taken for example) , we need a delay of $T_s = 1\mu s$. The length of the cable L needed to obtain this delay can be calculated as follows:

$$L = vT_s \tag{3-27}$$

where v is the velocity with which the signal travels in the cable The design features of an RF cable used in IMEC laboratory is given in appendix (B) and from the table we can see that the velocity of propagation is given as 77 percent of speed of light. Therefore, $v = 2.31 * 10^8$. Hence the required length of the cable is L = 231 meters.
In appendix (C) a "Specific Test Report" is provided for the RF cable used in IMEC laboratory, from the table we can see that, for a frequency range of 0.05-1.84 GHz, the

power dissipation is -0.3610 db/m and for frequency range of 1.84-3.64 GHz the power dissipation is -0.5284 db/m. Therefore, for an operating frequency of 1 GHz the total power dissipation would be 23.27 dbW. Therefore, it is highly impractical to implement this architecture. With this analysis we can say that the architecture 2 outperforms architecture 1 in terms of power consumption.

3-5 Summary

In this chapter, two different architectures for demodulating BPSK and DPSK signals using super regenerative receiver were introduced. In the first architecture (architecture 1), a DPSK signal is converted into an OOK signal using a delay circuit and an adder and then the conventional super regenerative receiver architecture is used to detect the OOK symbols. A mathematical analysis was done to obtain the expression for error probability, and the bit error rate curve obtained. In the second architecture (architecture 2), the BPSK and DBPSK signals were passed through the super regenerative receiver without converting them to OOK signals. The two architectures are compared based on performance and power. On comparing the performance obtained for architecture 2 with the first one we can conclude that, architecture 2 has better performance of about 5 db compared to the first one. In terms of power, from the above power analysis we can also conclude that architecture 1 is an impractical to implement and the total analog power consumed by architecture 2 is about 1.08 m W for an operating frequency of 2.4 GHz which outperforms architecture 1.

Chapter 4

Synchronization in Super Regenerative receivers

4-1 Introduction

The main principle of the super regenerative receiver is based on the theory of quenching. As explained in chapter (2), the quench oscillator causes periodic build up and decay of oscillations, the oscillations are maximum at the zero crossing where the quench signal goes towards the positive half cycle. If the quench signal has small phase errors then, the positive going zero crossings will not correspond to the maximum value in the carrier. As explained in the signal model in section (2-1) in chapter (2), the relationship between the quench frequency(f_q), data rate(R_b) and the carrier frequency(f_c) can be written as: $f_c = \mathrm{m}\ R_b$, $f_c = \mathrm{n}\ f_q$ and $f_q = \mathrm{q}\ R_b$ where m, n and q are positive integers. As shown in figure 4-2, the red coloured quench signal has no phase errors, at the end of the quench period, at t=$5 * 10^{-}5$ s, the amplitude of the carrier is 1V. The black coloured quench signal has a small phase error, so the positive going zero crossing of the quench cycle (at time $5.05 * 10^{-}5$ s) corresponds to the carrier amplitude of 0.9511 volts. For carrier frequencies much greater than the quench frequency, a small phase variation in the quench signal will result in large variations on the carrier. Therefore, it is very important for the quench signal to be accurately synchronized to the carrier at the peak points (for zero carrier phase).
The phase errors in the quench signal are due to the phase/timing jitter generated at the output of the quench VCO. Therefore, from the performance point of view, it is also important to analyse the effects of phase and timing jitter on the detection performance. In this chapter, the synchronization process using a phase locked loop is explained and also a mathematical analysis is done for obtaining the relation between the phase/timing jitter and the detection performance.

4-2 Receiver System model

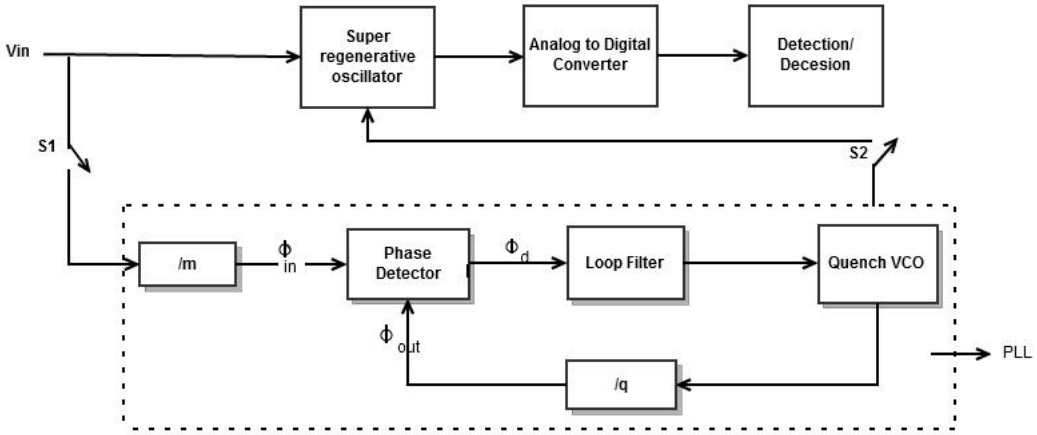

Figure 4-1: Receiver Model

The block diagram of the receiver model are shown in figure 4-1. It consists of a Super Regenerative Oscillator, PLL, Analog to Digital converter and a Decision Device to detect the received bits.
Th PLL block comprises of a frequency divider ($\div m$) where the incoming carrier frequency is divided to the data rate ($R_b = f_c/m$) and fed to the phase detector. The output of the phase detector is passed through a loop filter followed by the quench VCO, and the output of the quench VCO is fed back to the phase detector via a frequency divider ($\div q$) where the quench frequency is divided to the data rate ($R_b = f_q/q$). The PLL synchronises the quench VCO to the transmitter data clock and since the data rate is an integer multiple of the carrier frequency, the quench is also synchronized to the carrier phase.

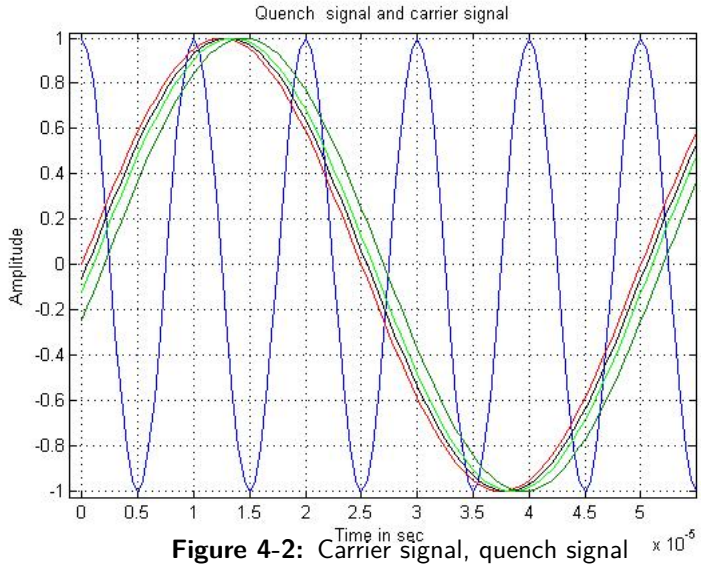

Figure 4-2: Carrier signal, quench signal

At the receiver, the switch S1 shown in the figure 4-1, initially connects V_{in} to the frequency divider block of the PLL. Considering a no noise scenario, the signal $v_i(t)$ applied to the input of the phase detector is given by

$$v_i(t) = V\cos(2\pi R_b t + \phi) \tag{4-1}$$

where $\phi = \frac{\phi_c}{m}$, ϕ_c is the carrier phase, R_b is the data rate explained in section (2-1). If the quench signal $v_q(t)$ has a phase shift ϕ_q then the expression for the signal at the output of the $\div$q block $v_o(t)$ is written as

$$v_o(t) = \sin(2\pi R_b t + \phi_d) \tag{4-2}$$

where $\phi_d = \frac{\phi_q}{q}$. The output of the phase detector can be written as

$$v_e(t) = VK_d v_i(t) v_o(t) \tag{4-3}$$

where K_d is the gain of the phase detector. Substituting for $v_i(t)$ and $v_o(t)$ from (4-1) (4-2) in (4-3) and simplifying we get

$$v_e(t) = \frac{VK_d}{2}\left[\sin((4\pi R_b t + \phi_d + \phi) + \sin(\phi_d - \phi)\right] \tag{4-4}$$

This signal is passed through a loop filter which acts as a low pass filter and produces a control voltage proportional to the phase difference. Output of Loop filter is given by

$$v_{lf}(t) = -\frac{K}{2}[\sin(\phi_e)] \tag{4-5}$$

where $\phi_e = \phi - \phi_d$ is the phase error, K=V K_d K_{lf} and K_{lf} is the loop filter gain. The control signal v_{lf} is fed back to the quench VCO which in turn generates a signal such that the phase error will decrease in the next iteration. The output of the quench VCO is given by [19]

$$v_{vco}(t) = \sin[2\pi R_d t + \hat{\phi_d}] \tag{4-6}$$

$$\hat{\phi_d} = K_v \int_{-\infty}^{t} v_{lf}(\tau)\,\mathrm{d}\tau. \tag{4-7}$$

where K_v is the VCO gain which is defined in unit of Hz/V. Synchronization is achieved when the control voltage $v_{lf}(t)$ reduces to 0. Let K= K_d K_v, then the transfer function $H(s) = \frac{\phi_o ut}{\phi_i n}$ for the sync loop in figure 4-1 can be written as [20]

$$H(s) = \frac{qKL_1(s)}{s + KL_1(s)} \tag{4-8}$$

$$L_1(s) = K_{lf}\frac{1+\tau_2 s}{1+\tau_1 s} \tag{4-9}$$

where q is an integer used in the frequency divider block shown in figure (4-1), k_{lf} is the gain of loop filter, $L_1(s)$ is the loop filter transfer function as given in (4-9), loop filter

is a low pass filter that responds to the low frequency component and removes the high frequency component in (4-4), the parameters τ_1, τ_2 in the loop filter transfer function are design parameters given in [20] such that ($\tau_1 \gg \tau_2$), they control the bandwidth of the loop. Substituting for $L_1(s)$ in (4-8) and simplifying results in: [13]

$$H(s) = \frac{2\zeta\omega_n s - (\omega_n^2/K) + \omega_n^2}{s^2 + 2\zeta\omega_n s + \omega_n^2} \tag{4-10}$$

$$\omega_n = \sqrt{\frac{K}{\tau_1}} \tag{4-11}$$

$$\zeta = \frac{\tau_2 + 1/K}{2\omega_n} \tag{4-12}$$

where K = $K_d\ K_{lf}\ K_v$, ω_n is the natural frequency, ζ is the damping factor. Converting

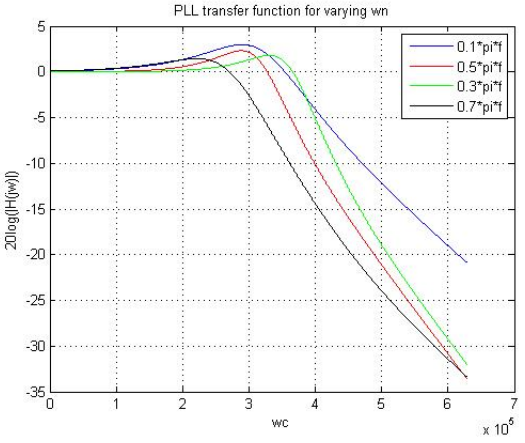

Figure 4-3: Transfer function of PLL when wn is varied

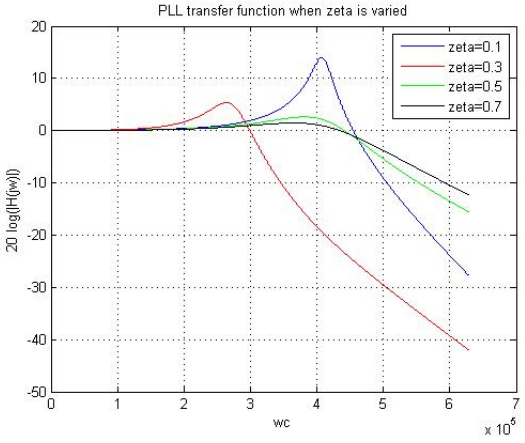

Figure 4-4: Transfer function of PLL when zeta is varied

the transfer function in (4-10)to its frequency response we get (put $s = j\omega$ and square $|H(j\omega)|$) we get

$$|H(j\omega)|^2 = \frac{\omega_n^4 + (2\zeta\omega_n\omega - \omega\omega_n^2/K)^2}{(\omega_n^2 - \omega^2)^2 + (2\zeta\omega_n\omega)^2} \tag{4-13}$$

The equivalent noise bandwidth of the loop can be written as [13]

$$B_{eq} = \frac{1}{2\pi|H(0)|^2} \int_{-\infty}^{\infty} |H(j\omega)|^2 \, \mathrm{d}\omega. \tag{4-14}$$

$$B_{eq} = \frac{(1 + (\tau_2\omega_n)^2)}{8\zeta\omega_n} \tag{4-15}$$

The synchronization loop acts like a low pass filter whose bandwidth is based on ω_n shown in figure 4-3, if it is large then the loop bandwidth is also large, fast tracking is possible but at the expense of more jitter due to noise. Low values of ω_n leads to narrow bandwidth, hence permitting less noise but at the expense of longer tracking

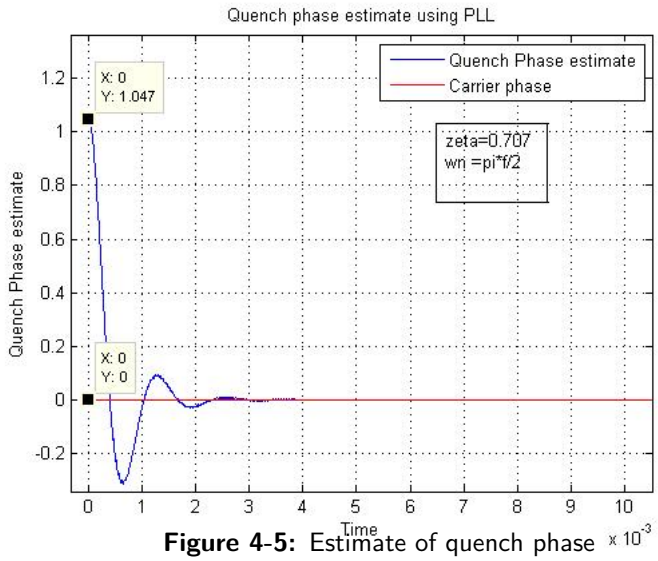

Figure 4-5: Estimate of quench phase

time. Figure 4-4 shows the PLL transfer function when ζ is varied. If the value of ζ is not used then the error signal do not damp out and the system becomes unstable.
The estimate of the quench phase when the carrier phase is zero is shown in figure 4-5. A switch S2 is used as shown in figure 4-1 gets connected to the SRO once the quench is synchronized, and switch S1 which was initially connected to the PLL, is detached. Since the synch loop will be in open circuit after synchronization, the noise voltage in the VCO may build up and may lose the frequency lock. To solve this problem we periodically run the phase locked loop so that synchronization errors caused by noise can be removed. Since the synchronization is performed based on preambles, we introduce these preambles at regular intervals in between the data so that synchronization can be maintained. This period depends upon the time taken by the noise in the VCO to build up and cause synch errors.

4-3 Relation between the phase jitter on the detection performance

As explained in section (4-1), a small phase variation in the quench signal would result in a large phase error in the carrier. These phase errors in the quench signal are due to the phase/timing jitter generated at the output of the quench VCO. In this section the effects of phase and timing jitter in the carrier caused due to the phase and timing jitter in the quench signal are discussed and also the relationship between phase jitter in the quench signal and BPSK detection performance is obtained.

The phase noise spectral density at the output of the VCO can be written as [19]

$$S_{\phi_q}(\omega) = S_{\phi_{in}}(\omega)|H(j\omega)|^2. \tag{4-16}$$

where $S_{\phi_{in}}(\omega)$ is the phase noise spectrum at the input of the PLL, $H(j\omega)$ is given in

(4-13). Substituting for $H(j\omega)$ in (4-16) we get

$$S_{\phi_q}(\omega) = S_{\phi_{in}}(\omega)\frac{\omega_n^4 + (2\zeta\omega_n\omega - \omega\omega_n^2/K)^2}{(\omega_n^2 - \omega^2)^2 + (2\zeta\omega_n\omega)^2} \tag{4-17}$$

Considering the noise at the input of the PLL to be additive white gaussian noise, the input phase noise spectral density can be written as $S_{\phi_{in}} = \frac{N_o}{2}$. Substituting this in (4-17) we get

$$S_{\phi_q}(\omega) = \frac{N_o}{2}\frac{\omega_n^4 + (2\zeta\omega_n\omega - \omega\omega_n^2/K)^2}{(\omega_n^2 - \omega^2)^2 + (2\zeta\omega_n\omega)^2} \tag{4-18}$$

Now the phase noise variance is defined by [21]

$$\sigma_{\phi_q}^2 = \frac{1}{2\pi}\int_{-\infty}^{\infty} S_{\phi_{in}}|H(j\omega)|^2\,\mathrm{d}\omega. \tag{4-19}$$

where $\frac{1}{2\pi|H(0)|^2}\int_{-\infty}^{\infty}|H(j\omega)|^2\,\mathrm{d}\omega.$ is called the equivalent noise bandwidth of the loop given in (4-14) Substituting for $S_{\phi_{in}} = \frac{N_o}{2}$ simplifying (4-19) we get

$$\sigma_{\phi_q}^2 = \frac{N_o|H(0)|^2}{2}\frac{(1 + (\tau_2\omega_n)^2)}{8\zeta\omega_n} \tag{4-20}$$

Substituting $\omega = 0$ in (4-13) we get $|H(0)|^2 = 1$. Therefore, the expression for phase jitter in the quench VCO in radians is given by

$$\sigma_{\phi_q} = \sqrt{\frac{N_o}{2}\frac{(1 + (\tau_2\omega_n)^2)}{8\zeta\omega_n}} \tag{4-21}$$

The time jitter at the output of the VCO due to the phase jitter in the input of the PLL is given by

$$\sigma_{\tau_q} = \frac{1}{2\pi f_q}\sqrt{\frac{N_o}{2}\frac{(1 + (\tau_2\omega_n)^2)}{8\zeta\omega_n}} \tag{4-22}$$

The phase jitter in the carrier signal obtained due to the phase jitter in the quench signal is then given by

$$\sigma_{\phi_c} = \omega_c\sigma_{\tau_q} \tag{4-23}$$

where ω_c is the carrier frequency. From equations (4-21) and (4-22) we can write $\sigma_{\tau_q} = \frac{\sigma_{\phi_q}}{2\pi f_q}$. Substituting this in (4-23) we get

$$\sigma_{\phi_c} = \frac{\omega_c}{\omega_q}\sigma_{\phi_q}\ \ rad. \tag{4-24}$$

Equation(4-24) represents the relation between the phase jitter in the carrier caused due to the phase jitter in the quench VCO. As explained in section (4-1), the carrier frequency is larger than the quench frequency, hence a small σ_{ϕ_q} in the quench signal would result in $\frac{\omega_c}{\omega_q}\sigma_{\phi_q}$ on the carrier. As given in [13], the probability density function for phase error ($\Delta\phi$) is given by

$$p(\Delta\phi) = \frac{exp(\gamma\cos(\Delta\phi))}{2\pi I_o(\gamma)} \tag{4-25}$$

Therefore probability of error (P_e) can be written as

$$P_e = 1 - \frac{1}{2\pi I_o(\gamma)} \int_{-\pi/2}^{\pi/2} p(\Delta\phi)\, \mathrm{d}\Delta\phi. \tag{4-26}$$

$$= 1 - \frac{\pi(L_o(\gamma) + I_o(\gamma))}{2\pi I_o(\gamma)}. \tag{4-27}$$

$$\tag{4-28}$$

where $L_o(x)$ is called 0^{th} order modified Struve function, $I_o(x)$ is the 0^{th} order Bessel function.

The relation between Signal to Noise ratio γ and the phase noise variance on the carrier $\sigma^2_{\phi_c}$ is given by

$$\gamma = 1/\sigma^2_{\phi_c} \tag{4-29}$$

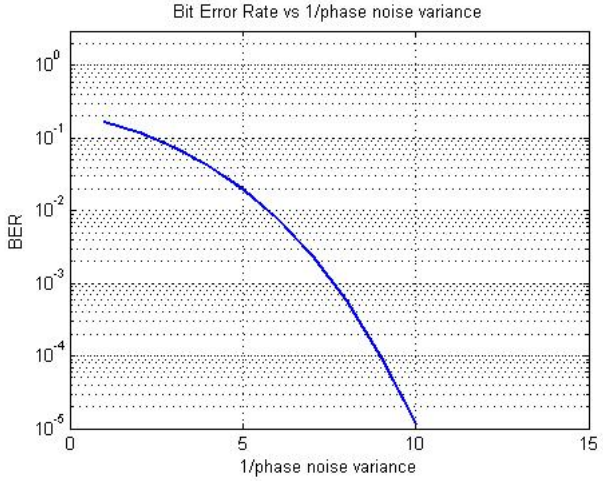

Figure 4-6: Bit error rate Vs Phase Noise Variance on the carrier

Figure 4-6 shows the bit error probability for BPSK vs $1/\sigma^2_{\phi_c}$. From the figure we can see that the higher the $1/\sigma^2_{\phi_c}$, the lower is the bit error rate. Therefore, for obtaining a BER about 10^-3, $\sigma^2_{\phi_c}$ should be about 0.1778 rad^2 and for obtaining a BER about 10^-5 $\sigma^2_{\phi_c}$ should be about 0.1 rad^2. Using (4-24), the required $\sigma^2_{\phi_c}$ can be achieved by reducing $\sigma^2_{\phi_q}$ given in (4-20), which means that the loop parameters such as the natural frequency, damping factor should be carefully designed so that it reduces the phase noise variance in the quench signal.

4-4 Summary

This chapter explains the synchronization process for super regenerative receivers. A phase locked loop technique is used for synchronizing the quench clock with the transmitter clock. The second part of the chapter provides a mathematical analysis for obtaining the relation between the phase/timing jitter of the quench signal and carrier

signal. Also the relation between the phase jitter in the carrier and the detection performance is provided. From this analysis it is concluded that, for proper detection, the phase jitter in the carrier should be within the range $0 \leq \sigma^2_{\phi_c} \leq 0.2rad^2$. This can be achieved by reducing $\sigma^2_{\phi_q}$ given in (4-20).

Chapter 5

Preamble detection techniques

5-1 Introduction

In digital communication systems, the detection circuit in the receiver decides the presence and the absence of a transmitted signal. This decision is usually based on comparing the received signal voltage with a predefined threshold. If the received signal voltage is greater than the threshold then the presence of the signal is confirmed. The signal that is transmitted is composed of three parts - preamble, header and payload. The preamble part mainly contains a SYNC field that provide information to enable the receiver to perform the necessary synchronization procedures, followed by a Start Frame Delimiter (SFD) field to indicate the end of the SYNC field and start of the data part. The header part usually contains signalling information like the modulation technique used at the transmitter, the time required to transmit the payload and CRC. The payload contains the actual data to be decoded. The problem statement here is to develop an algorithm for preamble detection for the given input settings. Given settings:

- Preamble length is 144 bits, which contains 128 bit SYNC field 16 bit SFD
- The SYNC field is having a sequence of logic 1's
- SFD field is having sequence $\{1111-1-1111-11-1-1-1-1-1\}$

In this chapter, an algorithm for preamble detection based on correlation and energy detection techniques are presented for the given input settings. Also the performance of signal detection, that can be measured using probability of detection and error probabilities like probability of missed detection and probability of false alarm are analysed.

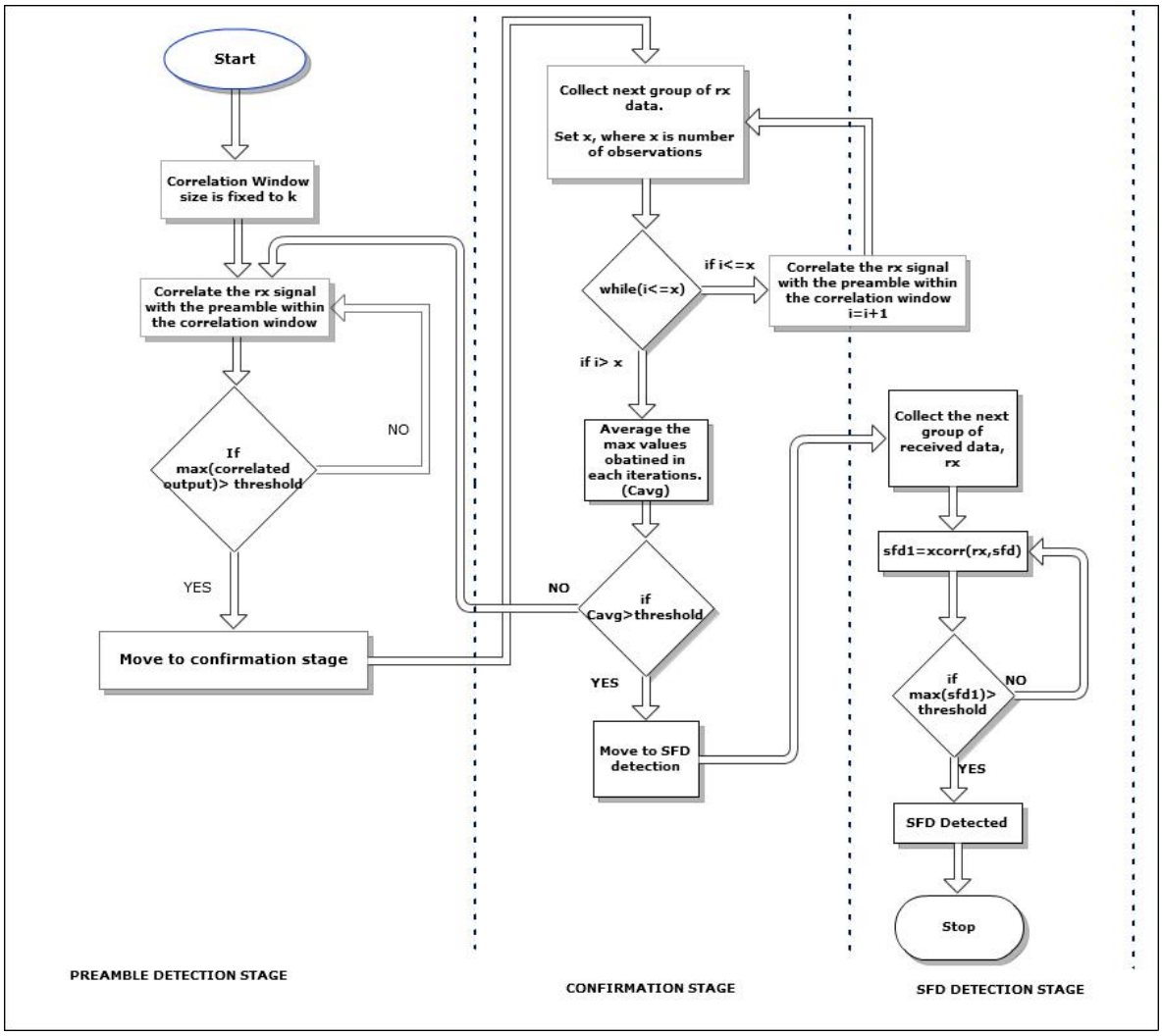

Figure 5-1: Flow chart for Signal detection stage, confirmation stage and SFD detection stage

5-2 Algorithm

Let us consider a packet structure shown in figure 5-2. The packet consists of the preamble part (SYNC, SFD) and payload. The total length of the packet is N bits, where the first L bits are preamble bits which are divided into a SYNC field of length P bits and an SFD field of length Q bits. The other $N - L$ bits comprise the payload. Figure (5-1)shows the flowchart for preamble detection for the given length of the preamble and its contents. The algorithm has three stages: SYNC detection stage, Confirmation stage and the SFD detection stage. The flowchart for the algorithm is shown in the figure 5-1. To begin with, the correlation window is initialized to a length say "k" bits, the incoming packets are buffered and grouped into k bits and threshold value is set for detection. In the SYNC detection stage, the receiver checks if the incoming signal is detected for the presence of any data. This detection can be done in two ways: a) Based on Correlation based (explained in section (5-2-1)) b) Based on

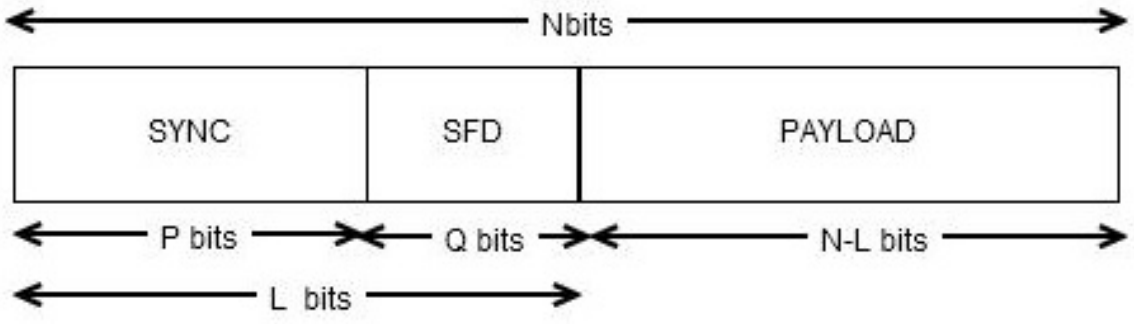

Figure 5-2: Packet structure

Energy detection (explained in section (5-2-5)). If the signal is detected, the system enters to the confirmation stage where the presence of data is confirmed. After this, the SFD sequence is searched in the received signal. Once the SFD sequence is detected, decoding of the payload starts.

5-2-1 Threshold setting

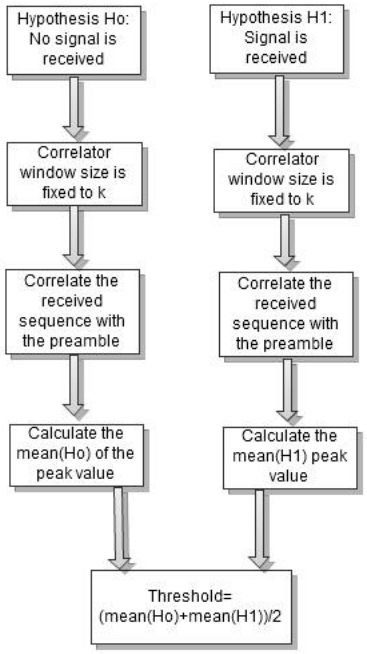

Figure 5-3: Flow chart for threshold estimation

The detection problem that is considered here is to differentiate between the following hypotheses:

$$H_0 : Y[n] = W[n] \tag{5-1}$$
$$H_1 : Y[n] = S[n] + W[n] \tag{5-2}$$

where $Y[n]$ is the received signal, which in the presence of data $S[n]$ will assume the form presented in H_1 and $W[n]$ is the additive white gaussian noise with zero mean and variance σ^2. The received signal $Y[n]$, in the presence of data, has a gaussian probability density function with mean μ variance σ^2.

$$p(y_s) = \frac{1}{\sqrt{2\pi\sigma^2}} e^{-} \frac{(y_s - \mu)^2}{2\sigma^2} \tag{5-3}$$

In the presence of noise with 0 mean and variance σ^2 only the distribution is given by

$$p(y_n) = \frac{1}{\sqrt{2\pi\sigma^2}} e^{-} \frac{y_n^2}{2\sigma^2} \tag{5-4}$$

In order to detect the presence of the signal, we correlate the received sequence with the known preamble, if the correlation peak is greater than a predefined threshold then the signal is said to be detected. For proper detection, the threshold should be determined correctly. The procedure of threshold detection is explained in the flowchart given figure (5-3)
Let x_k be the first k bits of the preamble sequence having a structure explained in section (5-2) and let y_k be the first k bits of the received sequence. The correlation output in the presence of the signal can be written as [13]

$$R_{xy}(m) = \sum_{n=1}^{2k-1} x(n)y(n+m) \tag{5-5}$$

$R_{xy}(m)$ reaches a maximum value when there are no lags i,e. $m = 0$. Therefore we can write

$$R_{xy}(0) = \sum_{n=1}^{k} x(n)y(n) \tag{5-6}$$

The probability density function of $R_{xy}(0)$ is given by

$$p(r_{xy}) = \frac{1}{\sqrt{2\pi\sigma_{R_{xy}}^2}} e^{-} \frac{(y_s - \mu_{R_{xy}})^2}{2\sigma_{R_{xy}}^2} \tag{5-7}$$

$$\mu_{R_{xy}} = \sum_{i=1}^{k} x(i)\mu_i \tag{5-8}$$

$$\sigma_{R_{xy}}^2 = \sum_{i=1}^{k} x^2(i)\sigma^2 \tag{5-9}$$

where $\mu_{R_{xy}}$ and $\sigma^2_{R_{xy}}$ are the mean and variance respectively. In the presence of noise only, Y[n] will be equal to W[n] as given in (5-1). Therefore, we can the write the probability density function of $R_{xy}(0)$ for hypotheses H_o as

$$p(r_n) = \frac{1}{\sqrt{2\pi\sigma^2_{R_{xy}}}} e^{-} \frac{r_n^2}{2\sigma^2_{R_{xy}}} \tag{5-10}$$

$$\tag{5-11}$$

this distribution is gaussian with mean 0 and variance same as $\sigma^2_{R_{xy}}$ given in (5-9). The threshold estimate is given by mid point between the means can can be written as

$$T_h = \frac{\mu_{R_{xy}}}{2} \tag{5-12}$$

5-2-2 SYNC detection and confirmation

In this stage, the arrival of the packet is detected at the receiver. The flowchart for detection is shown in the figure 5-1. The received signal is correlated with the first k bits of the preamble. If the peak value of the resulting signal crosses the threshold, then the signal is detected and the system will go into the confirmation stage, if the signal is not detected then the procedure is repeated again. The confirmation stage is basically used to confirm the detection of the signal and is shown in the flowchart in figure 5-1. The steps of the confirmation stage are same as for the detection stage except for the fact that the SYNC detection stage is executed several times and the peak value obtained in each iteration is averaged and this result is compared with the threshold. If this value is greater than the threshold then the system will move to SFD detection stage, else the system is looped back to the SYNC detection stage.

5-2-3 SFD Detection

In SFD detection, the known SFD sequence is correlated with the received packet. If the correlation result has a maximum value that exceeds the threshold then the SFD sequence is detected and from this point onwards the payload decoding process starts. If the maximum value of correlation is not longer than the threshold then the SFD search process repeats. The procedure for SFD detection is shown in the figure (5-1). A counter is initialized at the start of the SFD algorithm, it is incremented each time if the SFD is not detected. A maximum limit is set until which the SFD sequence search is to be done and this limit is given by $\max_{count}=\frac{len(preamble)}{k}$. When the counter value gets greater than max_{count}, then the system will restart the algorithm and the preamble search algorithm repeats. Figure 5-4 shows the simulation graph for SFD detection, from the figure we can see that the received signal is correlated with the SFD sequence at 260^{th} sample.

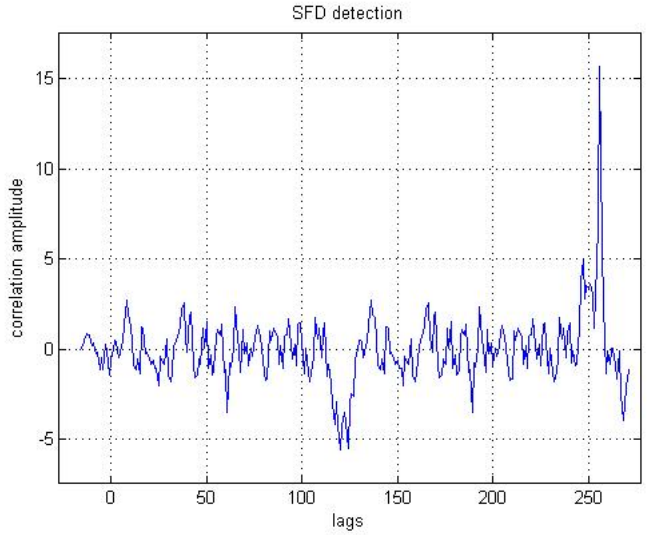

Figure 5-4: Correlation output for SFD detection

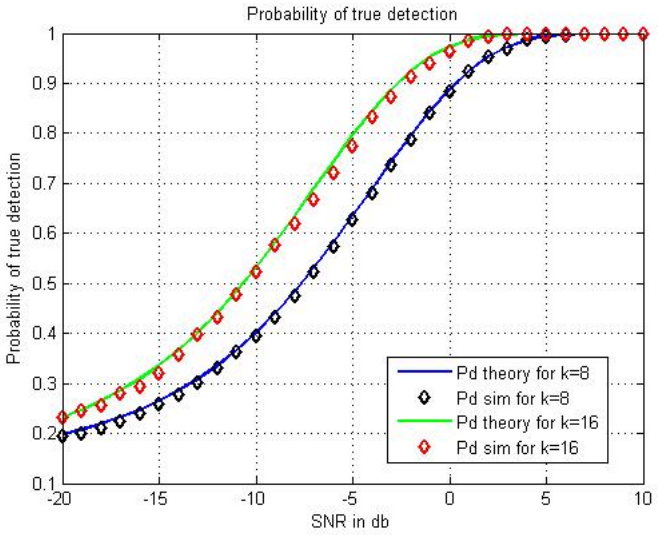

Figure 5-5: Probability of true detection

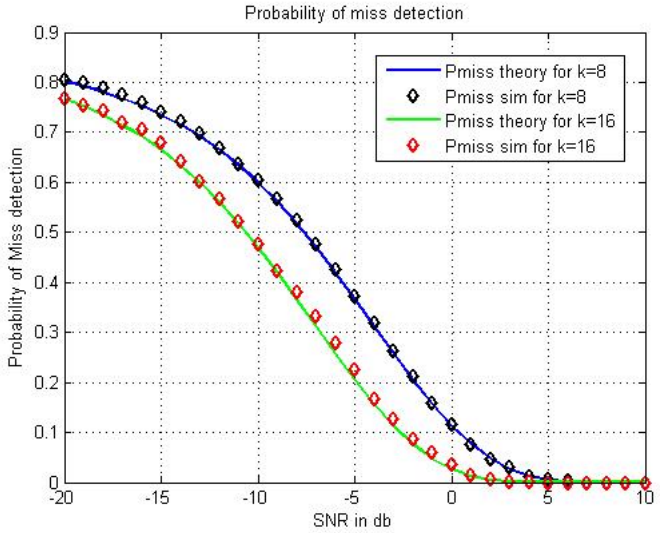

Figure 5-6: Probability of miss detection

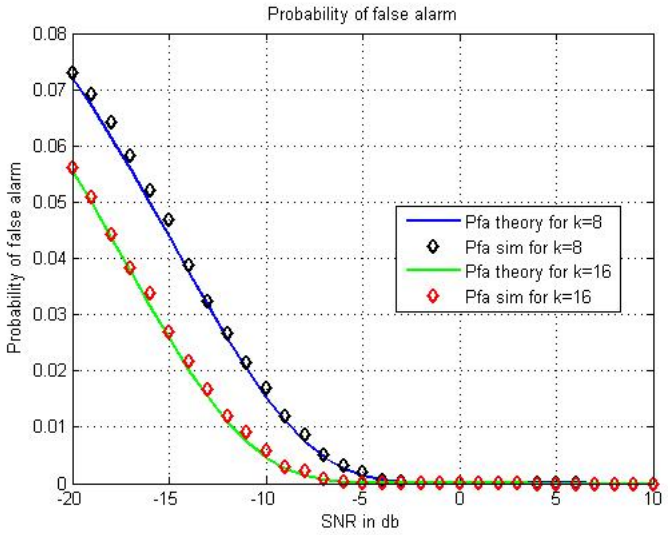

Figure 5-7: Probability of false alarm

5-2-4 Performance Analysis

The performance for signal detection is determined by the probability of detection and the error probabilities: probability of false alarm and probability of missed detection. The probability that the signal, when present, will be detected is called the probability of detection (P_d). The probability that a noise fluctuation will be mistaken for a signal is called the probability of false-alarm (P_{fa}). The probability at which the receiver wrongly detects or does not detect the transmitted symbols is called the probability of missed detection (P_{md}) [22]. Mathematically, the probability of detection and false alarm after the SYNC detection stage is given by,

$$P_d = \int_{T_h}^{\infty} p(r_{xy})\,\mathrm{d}r_{xy}. \tag{5-13}$$

$$P_{fa} = \int_{T_h}^{\infty} p(r_n)\,\mathrm{d}r_n. \tag{5-14}$$

Since we are using a preamble structure as explained in section (5-2), p_{rxy} given in (5-7) has mean and variance $\mu_{Rxy} = k$ and $\sigma^2_{Rxy} = k\sigma^2$ respectively, and p_{rn} has 0 mean and variance same as σ^2_{Rxy}. Substituting for $p_{r_{xy}}$ and p_{rn} from (5-7) and (5-10) in (5-13) and (5-14) respectively we get

$$P_d = \frac{1}{\sqrt{2\pi\sigma^2_{R_{xy}}}} \int_{T_h}^{\infty} e^{-} \frac{(r_{xy} - \mu_{R_{xy}})^2}{2\sigma^2_{R_{xy}}}\,\mathrm{d}r_{xy}. \tag{5-15}$$

$$P_{fa} = \frac{1}{\sqrt{2\pi\sigma^2_{R_{xy}}}} \int_{T_h}^{\infty} e^{-} \frac{r_n^2}{2\sigma^2_{R_{xy}}}\,\mathrm{d}r_n. \tag{5-16}$$

(5-15) and (5-16)can be simplified by applying the following transformations.

$$\text{Transformations for(5-15)} \begin{cases} z = \frac{r_{xy} - \mu_{Rxy}}{\sigma_{Rxy}} \\ dz = \frac{dr_{xy}}{\sigma_{Rxy}} \\ z = \frac{T_h - \mu_{Rxy}}{\sigma_{Rxy}} & \text{if } r_{xy} = T_h, \\ z = \infty & \text{if } r_{xy} = \infty. \end{cases} \tag{5-17}$$

$$\text{Transformations for(5-16)} \begin{cases} v = \frac{r_n}{\sigma_{Rxy}} \\ dv = \frac{dr_n}{\sigma_{Rxy}} \\ v = \frac{T_h}{\sigma_{Rxy}} & \text{if } r_n = T_h, \\ v = \infty & \text{if } r_n = \infty. \end{cases} \tag{5-18}$$

Then,

$$P_d = Q\left(\frac{T_h - \mu_{Rxy}}{\sigma_{Rxy}}\right) \tag{5-19}$$

$$P_{fa} = Q\left(\frac{T_h}{\sigma_{Rxy}}\right) \tag{5-20}$$

Substituting for T_h from (5-12), μ_{Rxy} and σ_{Rxy} in (5-19) and for T_h and σ_{Rxy} in (5-20) we get P_d and P_{fa} after detection of SYNC bits.

$$P_d = Q\bigg(- \frac{\sqrt{ki}}{2\sigma}\bigg) \tag{5-21}$$

$$P_{fa} = Q\bigg(\frac{\sqrt{ki}}{2\sigma}\bigg) \tag{5-22}$$

where σ is the standard deviation of noise. We know that signal to noise ratio γ can be written as $\gamma = \frac{V^2}{2\sigma^2}$. Therefore, we can write $\sigma = \sqrt{\frac{V^2}{2\gamma}}$. Substituting for σ in (5-21) and (5-22) we get

$$P_d(SYNC) = Q\bigg(- \sqrt{\frac{k\gamma}{2V^2}}\bigg) \tag{5-23}$$

$$P_{fa}(SYNC) = Q\bigg(\sqrt{\frac{k\gamma}{2V^2}}\bigg) \tag{5-24}$$

where γ is the signal to noise ratio defined at the input of preamble detection stage. In the confirmation stage, the correlation is performed for several iterations and the maximum value obtained in each iteration is averaged and this result compared with the threshold. Assuming that i number of iterations are performed in the confirmation stage, the probability of detection and false alarm after confirmation stage can be written as

$$P_d(Conf) = Q\bigg(- \sqrt{\frac{ki\gamma}{2V^2}}\bigg) \tag{5-25}$$

$$P_{fa}(Conf) = Q\bigg(\sqrt{\frac{ki\gamma}{2V^2}}\bigg) \tag{5-26}$$

In the SFD detection stage, a known SFD sequence is correlated with the received signal. The probability of detection ($P_d(SFD)$) and probability of false alarm ($P_{fa}(SFD)$) for SFD detection stage will result in the same expression as derived for SYNC detection stage. The total probability of true detection and false alarm after SYNC detection and Confirmation stage can be written as [23]

$$\begin{aligned} P_d(SYNC + Conf) &= P_d(SYNC)P_d(Conf|SYNC) \\ &= P_d(SYNC)P_d(Conf) \end{aligned} \tag{5-27}$$

$$\begin{aligned} P_{fa}(SYNC + Conf) &= P_{fa}(SYNC)P_{fa}(Conf|SYNC) \\ &= P_{fa}(SYNC)P_{fa}(Conf) \end{aligned} \tag{5-28}$$

Now the total probability of detection $P_d(total)$ and false alarm $P_{fa}(total)$ obtained after all the three stages can be written as

$$\begin{aligned} P_d(Total) &= P_d(SYNC + Conf)P_d(SFD|SYNC + Conf) \\ &= P_d(SYNC)P_d(Conf)P_d(SFD) \end{aligned} \tag{5-29}$$

$$\begin{aligned} P_{fa}(SYNC + Conf) &= P_{fa}(SYNC + Conf)P_{fa}(SFD|SYNC + Conf) \\ &= P_{fa}(SYNC)P_{fa}(Conf)P_{fa}(SFD) \end{aligned} \tag{5-30}$$

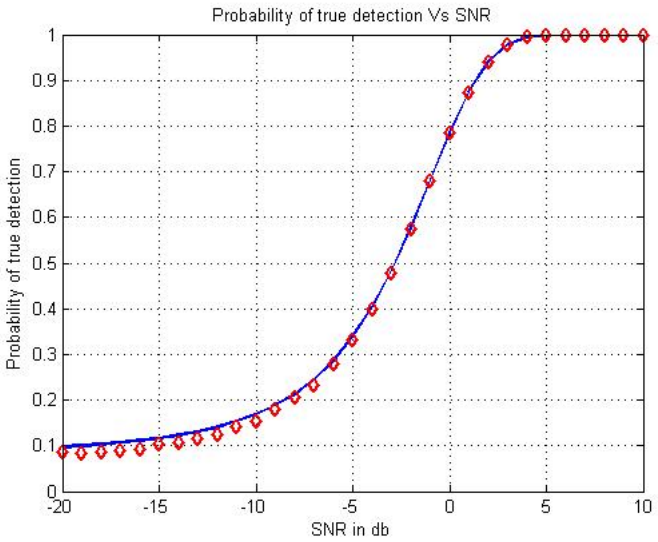

Figure 5-8: Probability of true detection

Writing (5-29) and (5-30) in terms of Q functions we get

$$P_d(Total) = Q\Big(-\sqrt{\frac{k\gamma}{2V^2}}\Big)Q\Big(-\sqrt{\frac{ki\gamma}{2V^2}}\Big)Q\Big(-\sqrt{\frac{k\gamma}{2V^2}}\Big) \tag{5-31}$$

$$P_{fa}(Total) = Q\Big(\sqrt{\frac{k\gamma}{2V^2}}\Big)Q\Big(\sqrt{\frac{ki\gamma}{2V^2}}\Big)Q\Big(\sqrt{\frac{k\gamma}{2V^2}}\Big) \tag{5-32}$$

Figures 5-5, 5-6 and 5-7 shows the plots for the total probabilities of detection, miss detection and false alarm for a correlation window size k = 8 bits and 16 bits. For correlation window size 8 bits SFD sequence $\{1-1-111-11-1\}$ is used.
From figure 5-5 we can see that if the window size "k" is longer then the probability of true detection increases, this is because as k increases the Q functions in the probability of detection increases as given in the expression (5-31). Also we observe that as SNR increases, the detection probability achieves a maximum value.
Figures 5-6 and 5-7 shows the missed detection probability ($P_{md}(total)$) and probability of false alarm, $P_{md}(total)$ is obtained from $1-P_d(total)$, from the figures we can observe that $P_{md}(total)$ for k=8 is higher than $P_{md}(total)$ for k=16. The same is observed for $P_{fa}(total)$.

5-2-5 Energy based SYNC detection

Section (5-2-2) explains correlation based SYNC detection where the received signal is correlated with the known SYNC bits in the preamble. Another technique for performing SYNC detection is by calculating the energy of the received signal, in this method the SYNC bits need not be known at the receiver. If the energy of the received signal rises above a pre-defined threshold, then we say that the SYNC is detected. The same algorithm explained in section (5-2) is followed, the only difference is that we perform

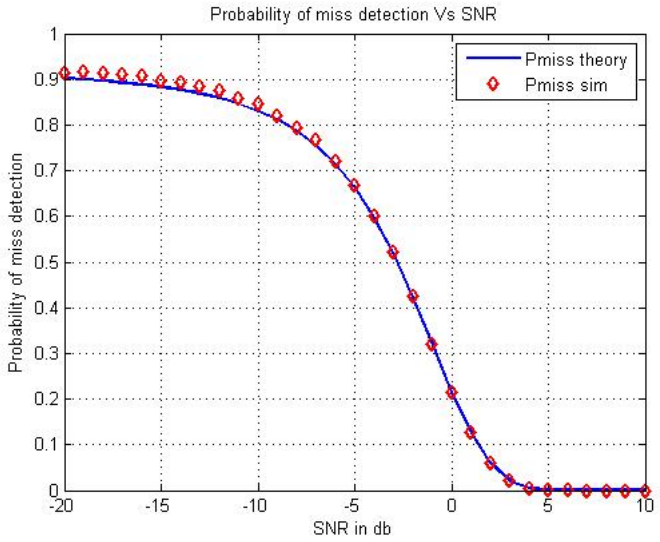

Figure 5-9: Probability of miss detection

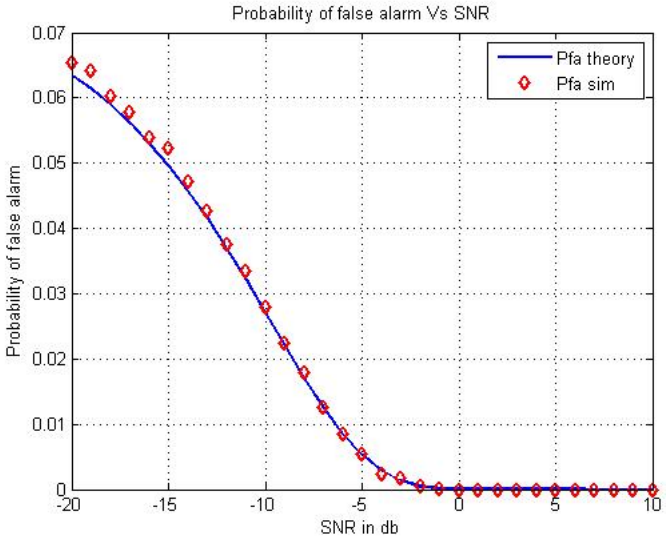

Figure 5-10: Probability of false alarm

energy based SYNC detection instead of correlation based SYNC detection. An optimum threshold (b_o) must be chosen so that it minimizes the total error probability. This threshold can be derived as follows.
As explained in section (5-2-1), let x_k be the first k bits of the preamble and let y_k be the first k bits of the received sequence. The energy detection output R_{y_k} can be written as [24]

$$R_{y_k} = \sum_{n=1}^{k} |y_k(n)|^2 \tag{5-33}$$

Therefore, the (R_{y_k}) has chi-squared distribution and non-central chi-squared distribution for hypothesis H_0 and H_1 respectively. As explained in [25], according to central limit theorem, (R_{y_k}) is asymptotically normally distributed if k is ≥ 20. Hence, we can model the statistic of (R_{y_k}) as

$$R_{y_k} \sim \begin{cases} \mathcal{N}(\mu_o, \sigma_o^2) & H_0, \\ \mathcal{N}(\mu_1, \sigma_1^2) & H_1 \end{cases} \tag{5-34}$$

where the values for μ_o, μ_1, σ_o^2, σ_1^2 are given as [13]

$$\mu_o = 2k\sigma^2 \tag{5-35}$$
$$\sigma_o = 4k\sigma^4 \tag{5-36}$$
$$\mu_1 = k(2\sigma^2 + V^2) \tag{5-37}$$
$$\sigma_1 = k(4\sigma^4 + 4\sigma^2 V^2) \tag{5-38}$$
$$\tag{5-39}$$

As explained in section (5-2-4), the expressions for P_{md} and P_{fa} can be written as

$$P_{md} = 1 - Q\left(\frac{b_o - \mu_1}{\sigma_1}\right) \tag{5-40}$$
$$P_{fa} = Q\left(\frac{b_o - \mu_o}{\sigma_o}\right) \tag{5-41}$$

The overall probability of error is the sum of the error probabilities P_{md} and P_{fa} and can be written as

$$P_e = 1 - Q\left(\frac{b_o - \mu_1}{\sigma_1}\right) + Q\left(\frac{b_o - \mu_o}{\sigma_o}\right) \tag{5-42}$$

The threshold b_o should be chosen such that it minimizes P_e, this can be done by partially differentiating P_e w.r.t b_o and equating it to 0 as shown below.

$$\frac{\partial Q\left(\frac{b_o-\mu_o}{\sigma_o}\right)}{\partial b_o} - \frac{\partial Q\left(\frac{b_o-\mu_1}{\sigma_1}\right)}{\partial b_o} = 0 \tag{5-43}$$

where, $\frac{\partial Q(x/a)}{\partial x} = -\frac{1}{\sqrt{2\pi\sigma^2}a} e^{-}(\frac{x^2}{2\sigma^2})$. Using this in (5-43) and simplifying we get

$$e^{-}\frac{1}{2}\left(\frac{b_o - \mu_o}{\sigma_o}\right)^2 = \left(\frac{\sigma_o^2}{\sigma_1^2}\right) e^{-}\frac{1}{2}\left(\frac{b_o - \mu_1}{\sigma_1}\right)^2 \tag{5-44}$$

Taking natural log on both sides and simplifying we get

$$\left(\frac{b_o-\mu_1}{\sigma_1}\right)^2-\left(\frac{b_o-\mu_o}{\sigma_o}\right)^2=2\log\left(\frac{\sigma_o^2}{\sigma_1^2}\right) \tag{5-45}$$

simplifying further we get

$$(\sigma_o^2-\sigma_1^2)b_0^2+2b_o(\mu_o\sigma_1^2-\mu_1\sigma_o^2)+\mu 1^2\sigma_o^2-\mu_o^2\sigma_1^2=2\sigma_o^2\sigma_1^2\log(\frac{\sigma_o^2}{\sigma_1^2}) \tag{5-46}$$

Substituting for μ_o, μ_1, σ_o^2, σ_1^2 in (5-46) and simplifying we get the expression for threshold b_o which minimizes the total probability for error

$$b_o=k\sigma^2+\sqrt{k^2\sigma^4+k^2\sigma^2V^2-\frac{8k\sigma^4}{V^2}(\sigma^2+V^2)\log\left(\frac{\sigma^2}{\sigma^2+V^2}\right)} \tag{5-47}$$

After SYNC detection, the probabilities of detection and false alarm can be written as shown in (5-19) and (5-20). During the confirmation stage, the energy of several SYNC packets are found, averaged and this result is compared with a threshold. Due to averaging the variances σ_o^2 and σ_1^2 will be reduced by a factor of number of averages. SFD detection is performed in the same way as explained in section (5-2-3). Figures 5-8, 5-9 and 5-10, shows the plots for total P_d, P_{md} and P_{fa} respectively for k=32. From the figure 5-8 we can see that as expected the probability of true detection increases as the SNR increases. From the plots of the probabilities of miss detection and false alarm, as expected, we observe the error probabilities reduces as SNR increases.

5-3 Summary

In this chapter, the algorithms for preamble detection based on correlation and energy are introduced and the performance for both techniques are analysed. Comparing the performance curves of both the techniques we can conclude that the total detection probability for correlation based SYNC detection is better compared to energy based detection.

Chapter 6

Conclusion and Future scope

6-1 Conclusion

In this thesis, a mathematical model for the super regenerative receiver for BPSK modulated signals in the presence of AWGN were discussed. Two architectures for demodulating BPSK and DPSK signals using super regenerative receiver were introduced. In the first architecture, a DPSK signal was converted into an OOK signal using a delay circuit and an adder and then the conventional Super Regenerative Receiver architecture was used to detect OOK symbols. In the second architecture, the BPSK and DPSK signals were demodulated using a super regenerative receiver without converting them to OOK signals. Both the architectures were compared based on performance and power and it was concluded that the second architecture is much better in terms of performance and power.
A system model for quench synchronization was presented and a mathematical analysis is done for obtaining the relation between the phase/timing jitter of the quench signal and carrier signal. Also the relation between the carrier phase jitter on the detection performance is provided. From this analysis it can be concluded that, for limiting the phase jitter, the loop parameters such as the natural frequency, damping factor, over all loop gain should be carefully designed so that it reduces the phase jitter in the quench signal.
Finally, algorithms for preamble detection based on correlation and energy techniques were introduced and the performance for both techniques was obtained. Comparing the performance curves of both techniques we can conclude that the total detection probability for correlation based SYNC detection is better compared to that of energy based detection. However, for energy based detection, the receiver does not need the prior knowledge of SYNC the bits.

6-2 Future Scope

- This project mainly focuses on analysis in an AWGN channel. The analysis of the proposed architectures can be extended for the case of fading channels.
- The mathematical analysis for super regenerative architectures are performed considering the input pulse shape to be rectangular. Different pulse shaped can be employed and their effects on synchronization can be analysed.
- The quench signal considered in this thesis is sinusoidal, various other quench signals could be employed and their effect on the detection performance can be analysed.
- It is worth while extending the current research for other PSK modulation schemes.

Appendix A

Receiver specifications 2.4 GHz and 1 GHz super regenerative receiver

A-1 Receiver specifications for 1 Mbps 2.4 GHz super regenerative receiver

Parameters	Data rate -1 Mbps	Unit
Supply Voltage	1.2	V
Reception center frequency	2.45	GHz
Quench shape	Sinusoidal	
-3 dB bandwidth	5	MHz
Sensitivity Level (BER= $10^{-}3$)	-92	dBm
IP3	-23	dBm
Leaked power at the antenna	-67	dBm

A-2 Receiver specifications for 100 kbps 1 GHz super regenerative receiver

Parameters	Data rate -100 kbps	Unit
Supply Voltage	1.2	V
Reception center frequency	1.032	GHz
Quench shape	Sinusoidal	
Quench frequency	1	MHz
Sensitivity Level (BER= $10^{-}3$)	-107.5	dBm
Leaked power at the antenna	-75	dBm

Appendix B

Cable design features

Cable design

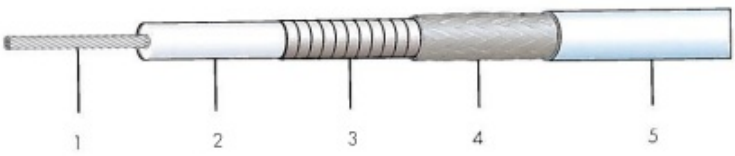

	Description	Diameter
1. Centre conductor	Stranded silver plated copper wire	
2. Dielectric	Low density PTFE	
3. 1st outer conductor	Silver-plated copper tape, wrapped	
4. 2nd outer conductor	Silver-plated copper braid	
5. Jacket	Fluoroethylenepropylene, blue	5.50 mm

Electrical cable data

Impedance					50 Ohm
Operating frequency					26.5 GHz
Capacitance					87 pF/m
Velocity of propagation					77 %
Time delay					4.3 ns/m
Nom. attenuation*	coefficient a	0.2930	coefficient b	0.0175	
Max. attenuation*	coefficient a	0.3223	coefficient b	0.0192	
Max. operating voltage					2.4 kVrms
Min. Screening effectiveness up to 18 GHz					90 dB

*Attenuation calculation $\alpha_{25} = a \cdot \sqrt{f}$ (GHz) + b·f (GHz) (dB/m)

General cable data

Temperature range	-55...+125 °C
Weight	6.9 kg/100m
Min. bending radius static	16 mm
Min. bending radius dynamic	25 mm

Figure B-1: Cable design features

Appendix C

Specific Test Report

Specific Test Report

Frequency Range [GHz]	IL min S21 [dB]	RL max S11 [dB]
0.05000 - 1.84500	-3.610	-21.963
1.84500 - 3.64000	-5.284	-33.697
3.64000 - 5.43500	-6.628	-30.379
5.43500 - 7.23000	-7.807	-28.658
7.23000 - 9.02500	-8.946	-23.103
9.02500 - 10.82000	-10.020	-23.456
10.82000 - 12.61500	-11.013	-27.319
12.61500 - 14.41000	-11.937	-27.011
14.41000 - 16.20500	-12.848	-25.513
16.20500 - 18.00000	-13.715	-21.817

Type:	SF104PEA-26.5/2X11SMA451/10M
Art no.:	AGSF104P
Serial no.:	500476 /4PEA
PA no.:	70899
Ring no.:	
Cable length:	10 m
Test length:	m
Connector 1:	SF_11_SMA-451
Connector 2:	SF_11_SMA-451
Cable:	SUCOFLEX_104_PE
Meas. System:	N5230C,MY49001834,A.09.42.12
Time:	11:19:47 A
Date:	4/3/2012
Inspected by:	KK /111
Start Freq.:	0.05000 GHz
Stop Freq.:	18.00000 GHz
Meas Points:	801
Source Power:	-10 dBm

Remarks: VK 385840/1 Temp. 23°C

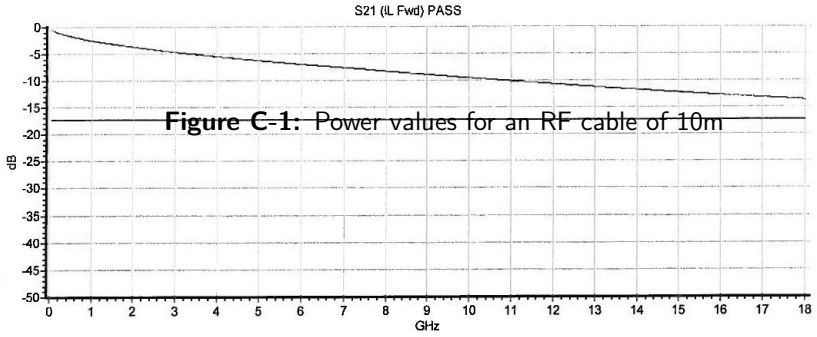

Figure C-1: Power values for an RF cable of 10m

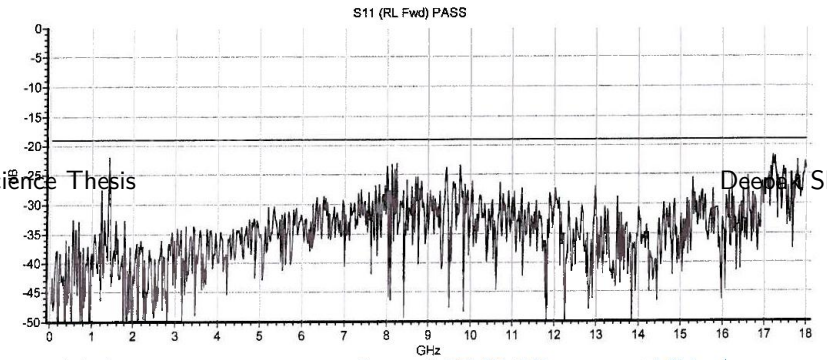

RF Technology Phone +41 (0)71 353 41 11 info@hubersuhner.com

H+S 84042165

Bibliography

[1] E. Armstrong, "Some recent developments of regenerative circuits," *Proceedings of the Institute of Radio Engineers*, vol. 10, no. 4, pp. 244 – 260, aug. 1922.

[2] U. Rohde and A. Poddar, "Super-regenerative receiver (srr)," in *Electron Devices and Solid-State Circuits, 2007. EDSSC 2007. IEEE Conference on*, dec. 2007, pp. 263 –266.

[3] I. Wikimedia foundation, "Receiver (radio)," June 2012. [Online]. Available: http://en.wikipedia.org/wiki/Receiver_(radio)#cite_note-3

[4] ——, "Regenerative circuit," May 2012. [Online]. Available: http://en.wikipedia.org/wiki/Regenerative_radio_receiver

[5] B. P. Otis, "Ultra-low power wireless technologies for sensor networks," Ph.D. dissertation, UNIVERSITY OF CALIFORNIA, BERKELEY, Spring, 2005.

[6] F. Moncunill, O. Mas, and P. Pala, "A direct-sequence spread-spectrum super-regenerative receiver," in *Circuits and Systems, 2000. Proceedings. ISCAS 2000 Geneva. The 2000 IEEE International Symposium on*, vol. 1, 2000, pp. 68 –71 vol.1.

[7] L. Hernandez and S. Paton, "A superregenerative receiver for phase and frequency modulated carriers," in *Circuits and Systems, 2002. ISCAS 2002. IEEE International Symposium on*, vol. 3, 2002, pp. III–81 – III–84 vol.3.

[8] F. Xavier Moncunill-Geniz, P. Pala-Schonwalder, F. del Aguila-Lopez, and R. Giralt-Mas, "Application of the superregenerative principle to uwb pulse generation and reception," in *Electronics, Circuits and Systems, 2007. ICECS 2007. 14th IEEE International Conference on*, dec. 2007, pp. 935 –938.

[9] J. Ayers, N. Panitantum, K. Mayaram, and T. Fiez, "A 2.4ghz wireless transceiver with 0.95nj/b link energy for multi-hop battery-freewireless sensor networks," in *VLSI Circuits (VLSIC), 2010 IEEE Symposium on*, june 2010, pp. 29 –30.

[10] F. Moncunill-Geniz, P. Pala-Schonwalder, and O. Mas-Casals, "A generic approach to the theory of superregenerative reception," *Circuits and Systems I: Regular Papers, IEEE Transactions on*, vol. 52, no. 1, pp. 54 – 70, jan. 2005.

[11] P. Pala-Schonwalder, F. Moncunill-Geniz, J. Bonet-Dalmau, F. del Aguila-Lopez, and R. Giralt-Mas, "A bpsk superregenerative receiver. preliminary results," in *Circuits and Systems, 2009. ISCAS 2009. IEEE International Symposium on*, may 2009, pp. 1537 –1540.

[12] O. M.-C. F. X. Moncunill-Geniz and P. Palà-Schönwälder., "Demodulation capabilities of a dsss super-regenerative receiver." feb 2002.

[13] J. Proakis, *Digital Communications*, 4th ed. McGraw-Hill Science/Engineering/-Math, Aug. 2000.

[14] M. Schwartz, W. R. Bennett, and S. Stein, *Communication systems and techniques by Mischa Schwartz, William R. Bennett and Seymour Stein.* McGraw-Hill, New York, 1966.

[15] J. P. M. G. Linnartz and P. G. M. Baltus, "Theoretical model for maximum throughput of a radio receiver with limited battery power."

[16] F. Moncunill-Geniz, P. Pala-Schonwalder, C. Dehollain, N. Joehl, and M. Declercq, "An 11-mb/s 2.1-mw synchronous superregenerative receiver at 2.4 ghz," *Microwave Theory and Techniques, IEEE Transactions on*, vol. 55, no. 6, pp. 1355 –1362, june 2007.

[17] A. Vouilloz, M. Declercq, and C. Dehollain, "A low-power cmos super-regenerative receiver at 1 ghz," *Solid-State Circuits, IEEE Journal of*, vol. 36, no. 3, pp. 440 –451, mar 2001.

[18] J. M. R. Simone Gambini, "Design of low-voltage analog to digital converter in submicron cmos," University of California at Berkeley, Tech. Rep., 2007 Jan.

[19] D. H. Wolaver, *Phase Locked Loop Circuit design*, P. Hall, Ed. Prentice Hall, Englewood Cliffs,NJ„ 1991.

[20] C. Barrett, "Fractional/integer-n pll basics, technical brief swra029, wireless communication business unit, ti," Texas Instruments, Tech. Rep., August 1999.

[21] Maxim, "Clock (clk) jitter and phase noise conversion(application note 3359)," Maxim Integrated Products, Tech. Rep., 2004 Dec10.

[22] M. I. Skolnik, *Radar Handbook Third Edition*, M. I. Skolnik, Ed. McGraw-Hill, 22 jan. 2008.

[23] M. R. S. J. Schiller, *Probability and Statistics, Second Edition*, B. Gilson, Ed. Schaum's Outline, 2000.

[24] B. P. Lathi, *Signal Processing and Linear Systems.* Oxford University Press, 2000.

[25] Z. Wang, D. Qu, T. Jiang, and T. Jin, "Efficient discovery of spectrum opportunities via adaptive collaborative spectrum sensing in cognitive radio networks," in *Communications (ICC), 2011 IEEE International Conference on*, june 2011, pp. 1 –5.

Glossary

Acronym	Abbreviation
AM	Analog Modulation
ADC	Analog to Digital Converter
ASK	Amplitude Shift Keying
AWGN	Additive White Gaussian Noise
BER	Bit Error Rate
BPSK	Binary Phase Shift Keying
CRC	Cyclic Redundancy Check
DBPSK	Differential Binary Phase Shift Keying
EbNo	Energy per bit to Noise Ratio
LNA	Low Noise Amplifier
OOK	On Off Keying
PDF	Probability Density Function
PLL	Phase Locked Loop
PSK	Phase Shift Keying
QO	Quench Oscillator
RF	Radio Frequency
SFD	Start Frame Delimiter
SNR	Signal to Noise Ratio
SRO	Super Regenerative Oscillator
SRR	Super Regenerative Receiver
SYNC	Synchronization
TRF	Tunable Radio Frequency
VCO	Voltage Controlled Oscillator

List of Symbols

Symbols	Meaning
V	Maximum Amplitude of the signal
ω	transmitter carrier frequency in radians
ϕ_i	BPSK symbol phase
ζ_o	maximum amplitude of the quench signal
ω_o	Receiver operating frequency
$s(t)$	Sensitivity curve of the super regenerative receiver
σ^2_{SRO}	Noise variance at the output of the super regenerative oscillator
μ_{SRO}	Mean value at the output of the super regenerative oscillator
γ	Signal to Noise ratio
b_o	Threshold
I_o	Zeroth order modified bessel function
f_c	Carrier Frequency
f_q	Quench Frequency
R_d	Data rate
ω_n	Natural Frequency
ζ	Damping factor
L_o	Zeroth order modified Struve function
P_e	Total Probability of error
$\sigma^2_{\phi_c}$	Phase noise variance on the carrier
$\sigma^2_{\phi_q}$	Phase noise variance on the quench
P_d	Probability of detection
P_{md}	Probability of miss detection
P_{fa}	Probability of false alarm
R_{xy}	Correlation output